

Response to reviewer comments on “Free Tropospheric Aerosols at the Mt. Bachelor Observatory: More Oxidized and Higher Sulfate Content Compared to Boundary Layer Aerosols”

by Shan Zhou et al.

We thank the reviewers for their thoughtful comments. We have carefully revised the manuscript accordingly. Our point-to-point responses can be found below, with reviewer comments repeated in black and author responses in blue. Changes made to the manuscript are in quotation marks.

Author response to Anonymous Referee #1

This manuscript describes high resolution aerosol chemistry measurements made at the mount bachelor’s observatory (MBO) during two periods in July and August of 2013. Aerosol chemistry and size distributions were measured using a high resolution aerosol mass spectrometer, and were operated alongside instruments characterizing gas-phase properties (NO_y, CO, O₃), and aerosol optical properties. As a result of its altitude and strong boundary layer dynamics the MBO site is often located in the free troposphere at night, providing the authors the opportunity to characterize FT composition. The objectives of this work were to describe the chemical and physical properties of FT aerosols and compare with those from the BL. This work is well prepared and described. The data set is a bit short and variable to generally describe FT aerosol FT aerosols.

General comments

1. How stable were the air mass sources during these two FT periods?

The sources of air masses during these two FT periods were quite stable based on 3-day back-trajectories calculated for air masses arriving at MBO every hour. Specifically, the clean periods mostly showed trajectories from the west, originating from the Pacific Ocean.

2. Page 5, Line 151: As discussed later on in the manuscript, this also suggest a supplementary source of sulfate aerosol particles in the FT, possibly from nucleation processes. Although no difference in the total mass of sulfate was observed during the day and night, were there differences in the signal ratios of the sulfate measured during the day (SO₄_BL) vs night (SO₄_FT).

The signal ratios among sulfate peaks, i.e., mass spectral fragmentation pattern of sulfate, are consistent throughout the entire campaign, thus nearly identical between the FT and BL. Note that there were differences in sulfate/NR-PM₁ ratio between day and night. As shown in figure 2 and discussed in the last paragraph of section 3.1., sulfate was the dominant PM₁ component at night whereas organic aerosol dominated PM₁ composition during daytime. The mean SO₄/NR-PM₁ ratio for FT periods (similar but not equal to nighttime) was 0.39, about 3.5 times of that for the BL periods (0.11).

3. The authors mention that the signal ratios of the sulfate peaks are similar to that of MSA. It is also mentioned that several sulfate peaks are associated with organic aerosols. Were there any trends in the PMF analysis that segregated the sulfate aerosol by diurnal patterns (the more oxidized OA vs the sulfate dominated OOA)? Were the signal ratios of the PMF sulfate factor similar to that of ammonium sulfate or similar to other types of sulfate.

The signal ratios of the sulfate peaks are actually different than those of MSA. In the PMF 3-factor solution, sulfate ions (i.e., SO_x⁺) were associated with two factors, the more oxidized OA and sulfate-dominated OOA. The diurnal profiles of these two factors are not identical, but both are flat in comparison with that of SV-OOA, which showed a strong daytime enhancement.

The ratios among sulfate ions in the two OOA spectra are nearly identical and both are highly similar to that of ammonium sulfate.

4. From the PMF(ORG+INORG), were nitrate peaks associated with any of the organics, and was the PMF analysis capable of extracting an organic nitrate (ON) factor that could be compared to the ON extracted using the Farmer et al., method?

As shown in Fig. S12, 78% of the NO^+ and NO_2^+ signals were associated with SV-OOA and the rest 22% were associated with the LV-OOA factor. Together with the high $\text{NO}^+/\text{NO}_2^+$ ratios, this result indicates that the nitrate signals observed during clean periods were predominantly contributed by organic nitrates, which is consistent with the Farmer et al method.

We have revised text in the 3rd paragraph of Section 3.3, which now reads:

“These findings, together with the fact that organonitrates were predominantly associated with SV-OOA (e.g., 78% of the aerosol nitrate signal was attributed to SV-OOA; Fig. S12), indicate that the SV-OOA observed in this study likely represented biogenic SOA formed at lower altitudes in the region and transported upward to the site by thermal winds during the day. ”

5. As shown in recent publications at both JFJ (Hermann et al., 2015) and at the PdD (Farah et al., 2018), the properties of FT aerosols can vary considerably depending on its last contact with the boundary layer. Similar analysis of air mass back trajectories on this data set would provide clear characteristics of FT aerosols at the MBO.

Hermann et al. (2015) and Farah et al. (2018) focused on characterizing aerosols in the free troposphere. Both studies used Lagrangian particle dispersion model to estimate the interaction of FT air mass with the BL and observed that particle number concentrations in the FT changed with time since the last contact with BL. While examining the influence of BL contact on FT aerosol characteristics at MBO would indeed be very interesting, using a Lagrangian particle dispersion model is beyond the scope of this work and analyzing the air mass back trajectories for this study may not work well since the trajectory model only allows for the estimation of time since last contact with BL every hour. In addition, the relatively short duration of this study period (~ 160 hours) may limit the statistical significance of the analysis results. Nevertheless, our approach of using water vapor mixing ratios to differentiate the FT and BL-influenced air masses is supported by extensive works previously conducted at MBO and serves well the goal of this present study, which focuses on characterizing chemical differences between aerosols in FT and in BL-influenced air masses. Details on the method are given in the first paragraph of section 3.4 and in Section 1 of the supplementary.

6. In the Hermann and Farah studies, the change in the size distribution for FT aerosols has been used as a tracer for FT air masses. In Figure 5, only average size distribution for the whole period are shown. Can the authors include the average size distributions for FT periods? Why are organic size distributions in the FT not included here? Can they be magnified? or are the signal to noise ratios too low?

We examined the average size distributions for both FT and BL-influenced periods. The size distributions of organic and sulfate in the BL-influence periods are shown in Fig. 5c. The size distribution of FT-sulfate is shown as well. However, the average organic size distribution during the FT periods is not shown because of low signal to noise ratio.

Herrmann, E.; Weingartner, E.; Henne, S.; Vuilleumier, L.; Bukowiecki, N.; Steinbacher, M.; Conen, F.; Collaud Coen, M.; Hammer, E.; Jurányi, Z.; et al. Analysis of long-term aerosol size distribution data from Jungfraujoch with emphasis on free tropospheric conditions, cloud influence, and air mass transport. *J. Geophys. Res. Atmos.* 2015, 120, 9459–9480.

Farah, Antoine; Freney, Evelyn; Chauvigné, Aurélien; Baray, Jean-Luc; Rose, Clémence; Picard, David; Colomb, Aurélie; Hadad, Dani; Abboud, Maher; Farah, Wehbeh; Seasonal variation of aerosol size distribution data at the Puy de Dôme station with emphasis on the boundary layer/free troposphere segregation, *Atmosphere*, 2018, 9,7,244.

7. For the comparison with other “altitude” sites, the authors could also take into account measurements from:

Minguillón, M.C., Ripoll, A., Pérez, N., Prévôt, A.S.H., Canonaco, F., Querol, X., Alastuey, A., 2015. Chemical characterization of submicron regional background aerosols in the western Mediterranean using an Aerosol Chemical Speciation Monitor. *Atmos. Chem. Phys* 15, 6379–6391. doi:10.5194/acp-15-6379-2015

Ripoll, A., Minguillón, M.C., Pey, J., Jimenez, J.L., Day, D.A., Sosedova, Y., Canonaco, F., Prévôt, A.S.H., Querol, X., Alastuey, A., 2015. Long-term real-time chemical characterization of submicron aerosols at Montsec (southern Pyrenees, 1570 m a.s.l.). *Atmos. Chem. Phys* 15, 2935–2951. doi:10.5194/acp-15-2935-2015

We thank the reviewer for recommending these references. The Ripoll et al. (2015) study, which was made at the summit of Montsec representing regional background conditions and covered mixed BL and FT periods in summer, has now been included in Fig. 6 and Table S1. However, we decide not to include the Minguillon et al. (2015) study, which took place on the upper slopes at an elevation of 720 m a.s.l. downwind of Barcelona urban areas, since its results are considered less representative of regional background conditions compared to the other high-altitude sites shown in Fig. 6.

8. Table S1, Figure 6: Why is there no NR-PM₁ mass concentrations for pdD 2012?

We have added the average NR-PM₁ mass from pdD 2012 in Table S1 and Figure 6.

9. Figure 6: O/C only 6/16 of the listed stations have values. Why so? It would be interesting to have this sort of overview of measurements? Can this information be obtained through making contact with the different stations?

The reason is that only 9 out of 16 of the listed studies used HR-AMS, out of which only 6 published the average O/C ratios. We contacted the authors/stations of the 3 studies to request average O/C ratios but received no response.

10. Figure 6: It seems strange that the puy de Dome has such high concentrations (higher than those in E.Asia (by a factor of 3!!)). Is this representative of the station or is it a particular period that was advected by unusual air masses.

We took a closer look at the puy de Dome study and found that the BL data during summer 2010 was probably not representative of the average summertime BL aerosols at Puy de Dome. The study only covered one week of sampling and 80% of the air masses arriving at the site were from the more polluted continental sector. We have replaced it with the data collected for the same site during the 2012 winter campaign, which appeared to be more representative of the wintertime BL aerosol at the site. Figure 1, Table S1, and relevant texts throughout the manuscript have been updated.

Minor comments:

Page 2, Line 35: This statement is important and useful, but can the authors include some references based on recent simulations that show the need to improve our knowledge of regional and FT aerosol in order to improve chemistry transport models?

We deduced the importance of properly representing FT aerosol chemistry in models. This sentence has now been revised:

“A quantitative understanding of aerosol properties and processes in regional background air masses and in the FT would be useful for improving chemical transport models and global climate simulations.”

Page 6, Line 187, and Page 7, Line 239 (and elsewhere): Can you provide the m/z values for each of these fragments.

The m/z values for ion fragments have been added throughout the manuscript.

Page 7, Line 226: The m/z 91 can also be associated with fragments of primary anthropogenic OA. How can the authors be sure that this fragment is solely biogenic? It has previously been illustrated that the situation of the f_{44} and f_{43} on the triangle plot could indicate the source/type of the aerosol, with biogenic aerosols being situated on the right hand side of the triangle (Jimenez et al., 2009; Ng et al., 2010). Can this be illustrated and commented in Figure S13.

It is true that m/z 91 can also be associated with fragments of primary anthropogenic OA and that the mass fraction of m/z 91 to total organic (f_{91}) is not a unique tracer for BSOA (Ng et al., 2011). However, in unpolluted biogenic-rich environment, f_{91} is useful for evaluating formation pathways of BSOA (Lee et al., 2016). Anthropogenic emissions have a negligible influence on MBO during this study and this conclusion is supported by aerosol composition measurements.

We have revised the discussions about f_{91} in the revised manuscript and the 3rd paragraph of Section 3.3. now reads:

“The SV-OOA spectrum showed a significant $C_7H_7^+$ signal at $m/z = 91.055$ ($f_{C_7H_7^+} = 0.65\%$) and a spectral pattern highly similar to biogenic SOA observed from a plant chamber (Kiendler-Scharr et al., 2009). $C_7H_7^+$ was proposed as an indicator for the presence of β -pinene + NO_3 reaction products (Boyd et al., 2015) and elevated $f_{C_7H_7^+}$ was previously observed in the AMS spectra of biogenic SOA both in ambient air and in chamber experiments (Kiendler-Scharr et al., 2009; Sun et al., 2009; Robinson et al., 2011; Setyan et al., 2012; Budisulistiorini et al., 2015; Chen et al., 2015). In addition, as shown in Fig. S13a, the SV-OOA of this study situates along the right leg of the triangle defined by worldwide ambient OA in the f_{44} vs f_{43} space. It has been illustrated previously that the f_{44} vs. f_{43} triangle plot could be used to indicate the source/type of the aerosols and that biogenic OA usually situate on the right hand side of the triangle (Jimenez et al., 2009; Ng et al., 2010). These findings, together with the fact that organonitrates were predominantly associated with SV-OOA (e.g., 78% of the aerosol nitrate signal was attributed to SV-OOA; Fig. S12), indicate that the SV-OOA observed in this study likely represented biogenic SOA formed at lower altitudes in the region and transported upward to the site by thermal winds during the day.”

Figure 1: Can the authors identify the FT periods in Figure 1.

A color indicator has been added on the top of Figure 1 to signify FT and BL-influenced periods. The caption of Figure 1 has been updated accordingly.

Figure 2: NR-PM1 Composition. What does the y-axis represent here, I presume fractional contribution. Here we see that, at night, in the FT, more than 90% of the particle composition is SO_4 aerosols. In Figure 1, we observe this to be the case in only 2 of the 9 nights. Is this figure an average of all data shown in Figure 1?

The y-axis represents the fractional mass contribution, as noted in the figure caption. Figure 2 shows that at night, SO_4 aerosol contributed up to 70% of the NR-PM₁ composition. For time from 0 to 5 am, sulfate fraction was on average ~ 60% only. This is consistent with figure 1.

Figure S13: The main text refers to LV-OOA and SV-OOA, but in this figure the OOA are labeled BL-OOA and FT-OOA.

Thanks for spotting the inconsistency. Labels in Figure S13 have been changed to LV-OOA and SV-OOA.

Jimenez, J.L., et al. Evolution of organic aerosols in the atmosphere. *Science* 326, 1525–9. doi:10.1126/science.1180353

We have cited this reference.

Page 8, Line 264: Please include the ratios expected for acidic and for neutralized conditions. Why not include the NH₄ predicted to NH₄ measured plots?

Nitrate and chloride concentrations were negligible in the study period and a majority of the nitrate signal was likely contributed by organic nitrates. Thus, only sulfate was considered in the calculation of the predicted NH₄. In this case, Figure 4a serves in the same way as the scatterplot of NH₄ measured vs NH₄ predicted.

The following sentence has been added:

“An ammonium-to-sulfate equivalent ratio of 1 suggests neutral particles whereas a ratio significantly lower than 1 suggests acidic particles.

Anonymous Referee #2

The manuscript submitted by Shan Zhou and coauthors describes in detail a subset of a NR-PM1 aerosol chemistry dataset acquired at a high altitude sampling site, Mount Bachelor Observatory during the summer of 2013. It focuses on a few days where no apparent fire influence was observed at the site and uses this data to: Describe typical background summer conditions at MBO - Analyze how boundary layer dynamics modulate the chemical characteristics of the aerosol observed. It then puts these measurements into a larger context of other NR-PM1 measurements at high altitude sites as well as aircraft observations. The available field data presented is fairly sparse and this affects the robustness/representativeness of the conclusions, as discussed below. Nevertheless, the authors provide adequate context in most cases to support their findings. The technical quality of the analysis is excellent, and provides additional insights into sources composition that are often missing in comparable publications. Given that these are the first AMS measurements under background conditions at a key high altitude site in North America, these results are important and useful, despite the small coverage. The classification of air masses into BL/FT used in the manuscript is based on previous publications by the same authors and gives sensible results, although some more detail on the impact of the uncertainty of the assignment on the conclusions would be desirable. The summary of AMS observations at Mountain Sites is a useful addition and valuable for future high altitude studies. Also in this case the sample is at present fairly small, especially if one focuses on measurements that are clearly of free tropospheric air. May this publication help encourage further contributions.

Major comments:

Line 66: It would be useful to know what the criteria were to determine the clean/remote analysis periods. Line 118 mentions that <120 ppb CO and <25 Mm⁻¹ at STP were observed, but those seem more descriptive (it clearly worked) than prescriptive. Can the authors explain if this based on back trajectories? Chemical markers? Other?

The clean periods in this study were determined based on the AMS indicator for biomass burning influences, f_{60} , the fraction of $C_2H_4O_2^+$ ($m/z = 60.021$) signal over total OA. Data with f_{60} lower than 0.3% (Cubison et al., 2011) were classified as clean periods. Concentrations of CO and aerosol particles were very low during these periods. In addition, 3-day back trajectories suggest that the air masses arriving at MBO during the clean periods had very stable source, mostly from the west, originating from the Pacific Ocean.

To make these points clearer, we have revised the first paragraph of section 3.1., which now reads:

“While observations at MBO were made continuously from July 25 to August 25, for this work, we use only data from July 25 to 30 and August 17 to 21, 2013, which were classified as periods free of wildfire influence. The HR-AMS indicator for biomass burning influence, namely the fraction of $C_2H_4O_2^+$ ($m/z = 60.021$) signal over total OA (f_{60}), was used for differentiating wildfire influences. Periods with f_{60} below 0.3% (Fig. S6) likely received negligible influence from BB (Cubison et al., 2011), thus were classified as clean periods. As shown in Fig. 1, throughout the clean periods, the CO mixing ratio and submicron aerosol light scattering at 550 nm (σ_{550nm}) were below 120 ppb and 25 Mm⁻¹ at STP, respectively, similar to values previously observed at MBO under clean conditions (Fischer et al., 2011; Timonen et al., 2014). The site was influenced by transported wildfire plumes during the other periods of BBOP and air pollutant levels increased substantially, e.g., CO and σ_{550nm} increased by up to 8–10 times compared to the clean periods and NR-PM₁ reached up to 140 $\mu\text{g m}^{-3}$ (Zhou et al., 2017). Aerosol absorption data were available for the second clean period (August 17–21) and the average ($\pm 1\sigma$) EC mass concentrations were estimated to be only 0.04 (± 0.14) $\mu\text{gC m}^{-3}$, further indicating a lack of BB influences. Additionally, although winds at MBO showed a persistent westerly component (Fig. 1a and Fig. S7b), the bivariate polar plot of NR-PM₁

concentrations exhibited a dispersed profile (Fig. S7c), indicating regional sources of aerosols during the clean periods.”

Line 110: Given that the two factors found are in good agreement with the factors found in Zhou et al, 2017, it would seem that focusing on the temporal evolution of these two for the full six week deployment would be a good way to improve statistics, especially regarding the BL/FT split (which should not really depend on the presence or absence of additional BB aerosol). PMF analysis in the presence of very large BB plumes can be challenging, but the analysis presented in Zhou et al, 2017 seems robust enough that this could work, and considerably strengthen the findings regarding e.g. daily trends and average FT composition. So I would encourage the authors to consider this possibility.

We differentiate FT and BL-influenced air masses based on measured water vapor mixing ratio and CO concentration and classify periods with $H_2O(g) < 2.5 \text{ g kg}^{-1}$ and $CO < 80 \text{ ppb}$ as “FT air” and the rest as “BL-influenced air”. Therefore, the BL/FT split only applies to clean periods. In addition, due to substantially higher aerosol signals during BB influenced periods, we had to exclude some low loading periods ($Org < 1.5 \text{ ug m}^{-3}$) from the full-length PMF analysis in order to allow the model to convergence. Approximately half of the clean period data were included in the full-length PMF analysis as a result. Fig. S4 and Fig. S5 demonstrated that the temporal trends of the two regional background factors from both PMF analysis (clean periods only and full-length) correlated tightly. This suggest that results derived from clean periods are statistically significant and robust.

We have clarified this point by revising this section, which now reads:

“Furthermore, the time series and mass spectra of the SV-OOA and LV-OOA derived here agreed well with the two background OOAs derived from PMF analysis of the whole dataset, including the clean periods discussed in this study and the periods influenced by wildfires (Zhou et al., 2017) (Figs. S4 and S5; $r^2 > 0.9$).”

Line 151: The authors write that NH_4 and SO_4 are relatively comparable in the FT and BL, but this seems to contradict the acidity gradient described later (based on NH_4/SO_4 molar ratios), please clarify. Furthermore, the conclusion that the sources of SO_4 are the same in the FT and BL is not really supported by the different size distributions observed (and the explanation given there). Given that sulfate concentrations in the BL are going to be a strong function of BL height and FT exchange, a direct comparison of these concentrations is not very meaningful, suggest removing.

Thanks for point this out; we said it wrong. SO_4 mass concentration was comparable in the FT and BL (0.35 vs 0.33 ug/m^3) but NH_4 mass concentration in the BL was on average 1.6 times of that in the FT, therefore, yielding more acidic particles in the FT. In addition, the fact that SO_4 size distribution was different in FT than in BL-influenced air suggests different sources of SO_4 in the FT and BL. Related texts have been revised:

“In contrast, sulfate exhibited relatively constant concentrations (Fig. 1e) and a less pronounced diurnal pattern (Fig. 2). The weaker influence from BL evolution indicates similar sulfate concentrations in the BL and FT in the remote continental region of the western US. This is consistent with the relatively long atmospheric lifetime and the regional characteristics of sulfate particles.”

Line 166/Fig 2: Constructing diurnal profiles based on six days of data is less than ideal, and the trends are somewhat obscured by the different times at which the PBL rose above the sampling site . Again, I suggest extending the PMF analysis for the full length of the deployment (Line 220) to spot check at least for some of the variables the robustness of the trends shown. That might also allow to filter for days where the BL/FT switch happened at consistent times and hence improve the robustness of the aerosol trends

We agree that more data would help the statistics. This study covered more than 8 days of data, with a time resolution of 2.5-min or 5-min. There are a total of 2192 data points included in the diurnal analysis.

The box whisker plots of the diurnal profiles of aerosol species and properties were examined. The results suggest that the diurnal trends are robust. Figure 2 shows the median diurnal trends instead of the mean, which further lowers the influences from episodic events. In addition, we performed a separate PMF analysis covering the full 1-month duration of the study. Periods with organic concentration below $1.5 \mu\text{g m}^{-3}$, which hindered the model to converge, were excluded from PMF analysis (Zhou et al., 2017). Approximately $\sim 50\%$ of the data during the clean periods were included in the full length PMF analysis. Two background OOA were derived from the full length PMF analysis. The temporal trends and mass spectra of the SV-OOA and LV-OOA derived from this study (clean periods only) agreed well with the full length PMF results (Fig. S4 and S5). The diurnal profiles of SV-OOA and LV-OOA also highly resembled those derived from the full length PMF analysis. These results further support that the diurnal profiles shown in Fig. 2 are representative of the background aerosols at MBO.

Line 186: It should be mentioned that Lee et al, “Substantial secondary organic aerosol formation in a coniferous forest: observations of both day- and nighttime chemistry”, *Atmos. Chem. Phys.*, 16, 6721–6733, 2016, doi:10.5194/acp-16-6721-2016, reported the same trends in particulate organic nitrated at the Whistler “middle altitude site” with likely very similar forests sources as at MBO . The authors may also consider adding this dataset to Fig 6 as well, although the lower sampling altitude makes it less comparable to other high altitude observations.

We thank the reviewer for this suggestion. We have added the following text to the end of the paragraph: “Similarly, Lee et al. (2016) observed that organonitrates made a significant contribution to the secondary OA (SOA) mass in the coniferous forested regions at Whistler – a mid-altitude site in western Canada.”

With regard to the suggestion of including the dataset in Fig. 6, we chose not to considering that the dataset was obtained at a mid-mountain site at lower sampling altitude, thus is less comparable to the other mountaintop datasets shown in Fig. 6.

Line 196: The MSA analysis is well done and a nice addition to the manuscript. Are the authors aware of the study by Sorooshian et al, “Surface and airborne measurements of organosulfur and methanesulfonate over the western United States and coastal areas” *J. Geophys. Res. Atmos.*, 120(16), 8535–8548, doi:10.1002/2015JD023822, 2015? They measured MSA and OS at ground sites near MBO during the Summer of 2013 as well, and found broadly similar concentrations, consistent with MSA being made in the continental BL.

We thank the reviewer for this reference. We have added the following sentence at the end of the 2nd paragraph in Section 3.2:

“Sorooshian et al. (2015) measured MSA and organosulfates at inland ground sites near MBO and found broadly similar concentrations.”

We have also revised the last paragraph in Section 3.2., which now reads:

“Oceans are generally considered a dominant source of dimethyl sulfide (DMS) and therefore its oxidation product MSA. However, the Pacific Ocean is 195 km to the west of MBO whereas the bivariate polar plot of MSA revealed that high concentrations were associated with winds from the east and the south – the inland areas (Fig. S11). In addition, MSA concentrations showed a clear diurnal cycle with a substantial daytime increase (Fig. 2), which suggests significant sources from the PBL. Aerosols in the PBL over this region likely have negligible oceanic influences since the Cascades mountain range lies between the Pacific Ocean and Mt. Bachelor and may obstruct surface wind bringing marine emissions inland. These results suggest that the sources of MSA at MBO were mostly continental, where a wide range of terrestrial sources including soil, vegetation, freshwater wetland, and paddy fields can emit DMS (Watts, 2000 and references therein). Furthermore, the maximum MSA/SO₄ ratio in this study was ~ 0.081 , much

lower than those observed in marine aerosols (e.g., average = 0.23 in sub-Arctic North East Pacific Ocean (Phinney et al., 2006)). Similarly, lower MSA/SO₄ ratios were usually found in terrestrial regions, e.g., 0.01 - 0.17 in Fresno where MSA was mostly attributed to non-marine sources (Ge et al., 2012; Young et al., 2016), 0.007 - 0.15 along the Atlantic coast under continental influences (Zorn et al., 2008; Huang et al., 2017), and averages of 0.02 - 0.04 (maximum = 0.11) in California inland regions (Sorooshian et al., 2015).”

Section 3.4: The diurnal profiles show a fairly clear “transition zone” between FT and BL influence, and including/excluding those periods will likely strongly affect the averages found (see also Wagner et al, *Atmos. Chem. Phys.*, 15, 7085–7102, 2015 as an example on the difficulty of properly defining the top of the BL). Such an analysis, either based on the diurnal profiles themselves or on the uncertainty of their threshold criteria, would help strengthen the confidence in the reported averages and trends, especially for the FT data.

The segregation of FT periods and BL-influenced periods in this study was performed based on water vapor mixing ratio. As discussed in Section 1 in the Supplement, extensive work has been done at MBO to differentiate FT air from BL influenced air using water vapor mixing ratio. Weiss-Penzias et al. (2006) and Fischer et al. (2010) used percentiles of water vapor mixing ratio to identify FT and BL-influenced air masses. These same studies also used water vapor calculated from the 0 and 12 UTC National Weather Service soundings from Medford, Oregon and Salem, Oregon to determine a representative altitude for the air masses sampled at MBO. Reidmiller et al. (2010) used chairlift soundings of water vapor mixing ratios at Mt. Bachelor coupled with high-resolution NO_x data from MBO to determine a time of day when the BL influence began at the mountain summit. While all these studies focus on segregating FT and BL-influenced air masses during Spring, Ambrose et al. (2011) used sounding data from Medford to compare with water vapor distributions at MBO and obtained a seasonal mean water vapor mixing ratios for MBO FT data, which for winter, spring, summer, and fall seasons corresponded with WV < 3.28, < 3.28, < 5.4, and < 4.12 g kg⁻¹. Based on the same work by Ambrose et al. (2011), McClure et al. (2016) interpolated between the seasonal values into a monthly criterion. Zhang and Jaffe (2017) contributed to a more accurate monthly FT/BL isolation at MBO based on comparison of MBO water vapor distributions to the water vapor soundings from Medford and Salem, Oregon, at equivalent pressure level. The water vapor criterion for FT air masses at MBO refers to the cut points when equivalent monthly averages of the retained drier portion of the MBO data and the soundings were obtained. The FT/BL-influenced water vapor criterion for each month is 3.26, 2.64, 2.46, 2.55, 3.06, 4.25, 5.14, 5.23, 4.60, 4.36, 3.44, 2.97 g kg⁻¹ (from January to December).

The water vapor cut points for FT periods in July and August were 5.14 and 5.23 g kg⁻¹, respectively. However, Convection in summer enhances the vertical transport of air masses and creates a thicker entrainment zone. The top of the BL is therefore even more challenging to define. As FT air is drier than BL air, a lower water vapor threshold would reduce the influence of entrainment zone on “FT” isolation. Therefore, we applied a more stringent water vapor criterion, the driest (minimum) segregation value of 2.5 g kg⁻¹.

We have revised the first paragraph of Section 3.4 to clarify these points. It now reads:

“To further examine the differences between aerosols in the free troposphere and boundary layer, we segregate periods using measurements of water vapor (H₂O_(g)). Extensive work has been done to differentiate free tropospheric air from boundary layer-influenced air at MBO using water vapor chairlift soundings (Reidmiller et al., 2010) and other approaches (Weiss-Penzias et al., 2006; Fischer et al., 2010; Ambrose et al., 2011; McClure et al., 2016; Zhang and Jaffe, 2017), as discussed in more detail in Section 1 of the Supplement. Zhang and Jaffe (2017) established more accurate monthly H₂O_(g) criteria for FT air masses at MBO – 5.1 and 5.2 g kg⁻¹ for July and August, respectively, and associated FT air masses with low H₂O_(g) values. However, since convection in summer enhances vertical transport and creates a thicker

entrainment zone where BL mixed with FT, properly defining the top of BL is challenging (Wagner et al., 2015). To avoid the influences of the transition zone on FT, we used a more stringent $\text{H}_2\text{O}_{(\text{g})}$ criterion, 2.5 g kg^{-1} , which is the lowest monthly cut point reported in Zhang and Jaffe (2017). In addition, we explored the usage of the estimated BL height from HYSPLIT back trajectory analysis as the segregation criteria. A comparison between these two methods is available in Section 1 of the Supplement. After careful evaluation, we classify periods with $\text{H}_2\text{O}_{(\text{g})} < 2.5 \text{ g kg}^{-1}$ and $\text{CO} < 80 \text{ ppb}$ as “FT air” and the rest as “BL-influenced air”.

Line 275-278: This seems mostly speculative. MSA could also be oxidized further to sulfate and/or partition to the gas phase instead of being washed out. Consider removing/shortening.

We have revised and shortened the discussions. The paragraph now reads:

“MSA correlated with HR-AMS sulfate for different aerosol regimes with different slopes. As shown in Fig. 4b, BL-influenced aerosols showed a range of MSA/SO_4 ratios generally higher than FT aerosols. This may be attributed to higher MSA concentration near terrestrial sources in the BL. Indeed, airborne measurements of MSA in aerosol over the western US in summer 2013 have shown that MSA loading decreased with the increase of altitude (Sorooshian et al., 2015). Furthermore, as discussed later on, sulfate was likely produced in the FT during regional new particle formation and growth events, which may further contribute to lower MSA/SO_4 ratio in FT aerosols.”

Line 295-306: Again this seems fairly speculative. There is no discernible enhancement of small particles in the (fairly noisy) sulfate size distribution presented, which is still within the envelope of the BL size distribution. So preferential activation/wash out of larger particles would suffice to account for the observed differences and nucleation is not needed to explain the difference. So consider shortening/removing.

We have revised the discussion and the texts now read:

“A distinctly different size distribution was observed for sulfate-containing particles in the FT (Fig. 5c), which exhibited a prominent mode at $\sim 250 \text{ nm}$. One possible explanation is preferential activation/wash out of larger particles, and thus the reduction of sulfate signal in larger size (droplet) modes. Condensational growth of newly nucleated particles in the FT may be another possibility. Scavenging could result in low particle surface area, which facilitates new particle formation (NPF) in the FT. Although we did not observe NPF events in this study (due to instrumental limitations), in-situ NPF events have been frequently observed in the FT (e.g., Hallar et al., 2011; Hallar et al., 2013). Formation and growth of new particles have also been observed over broad regions in the FT (Tröstl et al., 2016). Condensation of gas-phase sulfate products on small FT particles could contribute to the observed condensation mode sulfate particles at MBO. These observations may shed light on the different sources and processes of aerosols in the BL and FT and suggest that sulfate and organic aerosols were likely present in both internal and external mixtures at MBO.”

Line 328-336: I am not following. If the average FT NH_4/SO_4 molar ratio is less than 0.3, the particles will be liquid bisulfate/sulfuric acid down to fairly low RH, hence the discussion of solid ammonium sulfate as presented does not seem really relevant to the findings. Please explain.

We have revised the discussion, which now reads:

“The extent to which sulfate particles are neutralized has major implications for aerosol radiative forcing. The average relative humidity at MBO was $25.6 (\pm 8.9) \%$ during the clean periods. Acidic sulfate aerosols are more hygroscopic than ammonium sulfate. The resulting increase in aerosol water content both increases the direct radiative forcing of sulfate (Adams et al., 2001; Jacobson, 2001) and promotes homogenous ice nucleation (Koop et al., 2000). In addition, while mineral dust particles coated with

ammonium sulfate are efficient ice nuclei, those coated with sulfuric acid can lose their ice nucleating ability (Eastwood et al., 2009).”

Minor comments:

Line 32: “At lower altitudes “ instead of “in lower altitudes”
Changed.

Line 39: While aircraft measurements are indeed expensive, I would argue that the main advantage of mountaintop observatories are long-term, continuous measurements that are invaluable for statistics. Obviously deploying complicated instrumentation such as the AMS can be a challenge for such sites as well, but I think it is worth mentioning this.

Agree. The following sentence has been added:

“Another main advantage of mountaintop observatories are long-term continuous measurements, which are invaluable for statistics.”

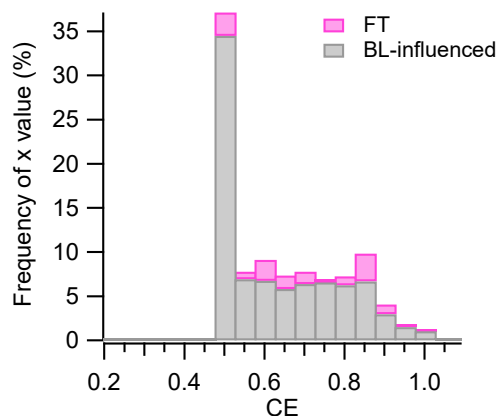
Line 40: Given the inclusion of the Whistler site, I would suggest replacing “US” with “North America”
Replaced.

Line 45: Suggest adding to your list of non-AMS particle measurements: L. Ahlm et al, “Temperature-dependent accumulation mode particle and cloud nuclei concentrations from biogenic sources during WACS 2010”, Atmos. Chem. Phys., 13, 3393–3407, 2013, doi:10.5194/acp-13-3393-2013
Added.

Line 82: “the established data analysis tool” instead of “established data analysis tool”
Changed.

Line 84: It would be useful to document the range of CEs observed. A histogram keyed by BL/FT influence would be appropriate, and would serve to highlight again the gradient in acidity between the different air masses sampled at MBO.

The composition-dependent collection efficiency ranged from 0.5 to 1 during this study. A histogram of the CE values colored by FT and BL-influenced periods is shown below. High CE was more frequently observed during FT periods, mainly because of acidic particles.



We have revised the text to read:

“A composition-dependent CE (ranging from 0.5 to 1; average = 0.66) was applied based on...”

Line 131: Is the chloride associated with periods of somewhat larger inorganic nitrate?

As Hu et al, Aerosol Sci. Technol., 51,735-754, doi:10.1080/02786826.2017.1296104 described, under such conditions chloride can be a vaporizer artifact, and is easily testable by reviewing the ammonium nitrate calibrations. Given the relative concentrations of chloride and nitrate, this is unlikely, but should be mentioned.

We didn't see elevated chloride signal associated with high nitrate mass. In fact, for most of the time during the clean periods, chloride signal was below limit of quantification (i.e., < 3 times of detection limit). We therefore removed the mentioning of chloride in aerosol composition. We have added the following sentence in the revised manuscript: "Chloride was close or below detection limit for most of the time during the clean periods."

Fig 4: Suggest adding a timeseries of the ratios, with the FT periods clearly marked, that would make the point(s) better than these correlation plots.

The time series of the ratios are shown below. We think the points we want to convey are more clearly illustrated in the scatterplots though.

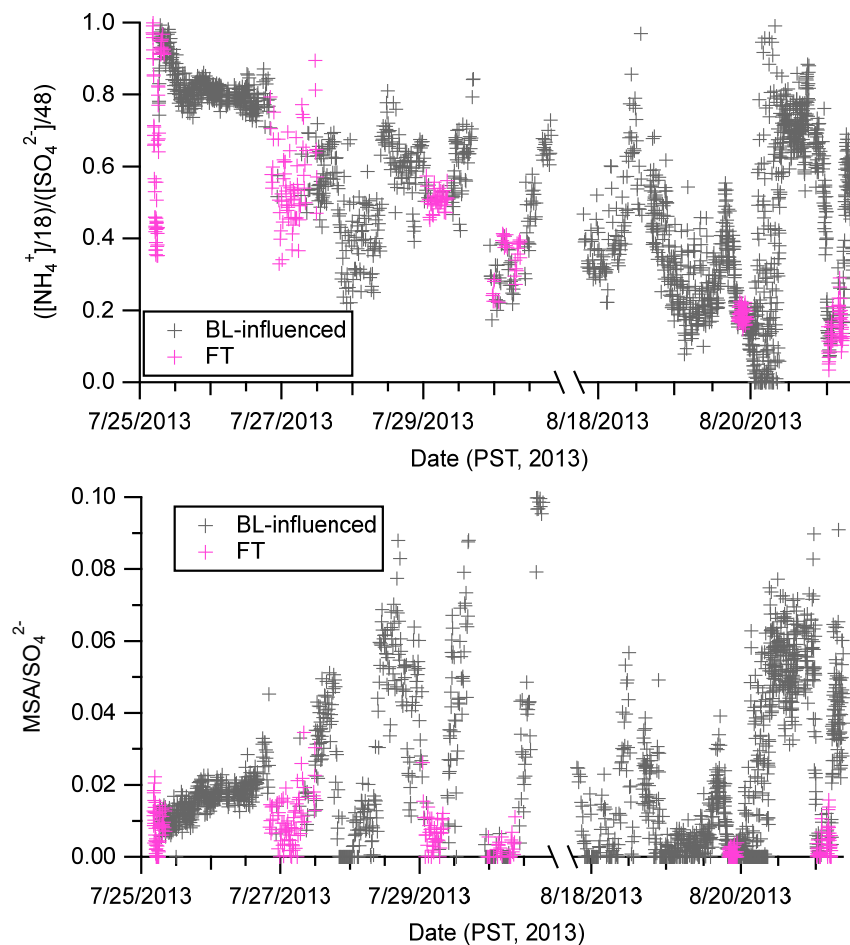


Fig S13 (middle): Please add the background line from Cubison et al. It looks like your factors lie pretty much right on top of it, as in Zhou et al, 2017.

Done as suggested. Yes, both factors situate to the left of the background line ($f_{60} = 0.3\%$).

References

- Ambrose, J. L., Reidmiller, D. R., and Jaffe, D. A.: Causes of high O₃ in the lower free troposphere over the Pacific Northwest as observed at the Mt. Bachelor Observatory, *Atmos. Environ.*, 45, 5302-5315, 2011.
- Fischer, E. V., Jaffe, D. A., Reidmiller, D. R., and Jaegle, L.: Meteorological controls on observed peroxyacetyl nitrate at Mount Bachelor during the spring of 2008, *J. Geophys. Res. Atmos.*, 115, 2010.
- Lee, A. K. Y., Abbatt, J. P. D., Leaitch, W. R., Li, S. M., Sjostedt, S. J., Wentzell, J. J. B., Liggio, J., and Macdonald, A. M.: Substantial secondary organic aerosol formation in a coniferous forest: observations of both day- and nighttime chemistry, *Atmos. Chem. Phys.*, 16, 6721-6733, 2016.
- McClure, C. D., Jaffe, D. A., and Gao, H.: Carbon Dioxide in the Free Troposphere and Boundary Layer at the Mt. Bachelor Observatory, *Aerosol Air Qual. Res.*, 16, 717-728, 2016.
- Reidmiller, D. R., Jaffe, D. A., Fischer, E. V., and Finley, B.: Nitrogen oxides in the boundary layer and free troposphere at the Mt. Bachelor Observatory, *Atmos. Chem. Phys.*, 10, 6043-6062, 2010.
- Sorooshian, A., Crosbie, E., Maudlin, L. C., Youn, J.-S., Wang, Z., Shingler, T., Ortega, A. M., Hersey, S., and Woods, R. K.: Surface and airborne measurements of organosulfur and methanesulfonate over the western United States and coastal areas, *Journal of Geophysical Research: Atmospheres*, 120, 8535-8548, 2015.
- Weiss-Penzias, P., Jaffe, D. A., Swartzendruber, P., Dennison, J. B., Chand, D., Hafner, W., and Prestbo, E.: Observations of Asian air pollution in the free troposphere at Mount Bachelor Observatory during the spring of 2004, *J. Geophys. Res. Atmos.*, 111, D10304, 2006.
- Zhang, L. and Jaffe, D. A.: Trends and sources of ozone and sub-micron aerosols at the Mt. Bachelor Observatory (MBO) during 2004–2015, *Atmos. Environ.*, 165, 143-154, 2017.

Free Tropospheric Aerosols at the Mt. Bachelor Observatory: More Oxidized and Higher Sulfate Content Compared to Boundary Layer Aerosols

Shan Zhou¹, Sonya Collier¹, Daniel A. Jaffe^{2,3}, Qi Zhang^{1*}

¹Department of Environmental Toxicology, University of California, Davis, CA 95616, USA

²School of Science, Technology, Engineering, and Mathematics, University of Washington Bothell, Bothell, WA, USA

³Department of Atmospheric Sciences, University of Washington, Seattle, WA, USA

Correspondence to: Qi Zhang (dkwzhang@ucdavis.edu)

Abstract

Understanding the properties and lifecycle processes of aerosol particles in regional air masses is crucial for constraining the climate impacts of aerosols on a global scale. In this study, characteristics of aerosols in the boundary layer (BL) and free troposphere (FT) of a remote continental region in the western US were studied using a high-resolution time-of-flight aerosol mass spectrometer deployed at the Mount Bachelor Observatory (MBO; 2763 m a.s.l.) in central Oregon in summer 2013. In the absence of wildfire influence, the average ($\pm 1\sigma$) concentration of non-refractory submicrometer particulate matter (NR-PM₁) at MBO was $2.8 (\pm 2.8) \mu\text{g m}^{-3}$ and 84% of the mass was organic. [The other NR-PM₁ components were sulfate \(11%\), ammonium \(2.8%\), and nitrate \(0.9%\).](#) The organic aerosol (OA) at MBO from these clean periods showed clear diurnal variations driven by the boundary layer dynamics with significantly higher concentrations occurring during daytime, upslope conditions. NR-PM₁ contained a higher mass fraction of sulfate and was frequently acidic when MBO resided in the FT. In addition, OA in the FT was found to be highly oxidized ([average O/C \$\sim\$ 1.17](#)) with low volatility. ~~In contrast, while OA associated within BL-~~ [influenced](#) air masses ~~had an was moderately oxidized (average O/C of 0.67) and semivolatile. There are indications that the BL-influence OA observed at MBO was more enriched of organonitrates and organosulfur compounds (e.g., MSA) and appeared to be semivolatile-representative of biogenic SOA originated in the BL. A summary of the chemical compositions of NR-PM₁ measured at a number of other high-altitude locations in the world is presented and similar contrasts between FT and BL aerosols were observed.~~ The significant compositional and physical differences observed between FT and BL aerosols may have important implications for understanding the climate effects of regional background aerosols.

1 Introduction

Atmospheric aerosols can scatter and absorb incident sunlight, therefore altering the radiation budget of the earth directly. Depending on their chemical composition and microphysical properties, aerosol particles can also act as cloud condensation nuclei and or ice nuclei and affect climate indirectly by altering the lifetime and optical properties

33 of clouds. Understanding the properties and the lifecycle processes of atmospheric aerosols is important for reducing
34 the uncertainties in aerosol climate forcing (Boucher, 2013)(Boucher, 2013).

35 Aerosols and their precursor gases are mostly emitted in the planetary boundary layer (PBL) but can be
36 transported into the free troposphere (FT) through convection and frontal uplift. In the FT, aerosols are subjected to
37 less efficient dry deposition and can have longer lifetimes than those ~~in at~~ lower altitudes, facilitating regional
38 recirculation or long distance transport (Jaffe et al., 2005a; Dunlea et al., 2009; Sun et al., 2009)(Jaffe et al., 2005a;
39 Dunlea et al., 2009; Sun et al., 2009). Under certain atmospheric conditions, aerosols in the FT can be entrained into
40 the BL, affecting remote regions where local emissions may be minimal (Schroder et al., 2002; Timonen et al., 2013;
41 Wang et al., 2016)(Schroder et al., 2002; Timonen et al., 2013; Wang et al., 2016). A quantitative understanding of
42 aerosol properties and processes in regional background air masses and in the FT ~~is necessary~~would be useful
43 for improving chemical transport models and global climate simulations.

44 High-altitude mountaintop observatories are important platforms for studying aerosols in regional ~~and FT~~ air
45 masses, ~~especially in the FT~~ without the added expense and difficulty of making airborne measurements. ~~Another~~
46 ~~main advantage of mountaintop observatories are long-term continuous measurements, which are invaluable for~~
47 ~~statistics.~~ Various mountaintop sites have been operated in ~~the US~~North America and Europe to perform long-term
48 measurements on aerosol optical properties, number, and size distributions and trace gases in continental background
49 air masses (Jaffe et al., 2005b; e.g., Van Dingenen et al., 2005; Reidmiller et al., 2010; Fischer et al., 2011; Hallar et
50 al., 2011; Rose et al., 2015; Bianchi et al., 2016; Hallar et al., 2016; Tröstl et al., 2016; Zhang and Jaffe, 2017)(Jaffe
51 et al., 2005b; e.g., Van Dingenen et al., 2005; Reidmiller et al., 2010; Fischer et al., 2011; Hallar et al., 2011; Rose et
52 al., 2015; Bianchi et al., 2016; Hallar et al., 2016; Tröstl et al., 2016; Zhang and Jaffe, 2017). Aerosol chemical
53 composition has also been studied from high elevation sites, through both filter collection followed by offline analysis
54 (e.g., Takahama et al., 2011; Hallar et al., 2013; Dzepina et al., 2015)(e.g., Takahama et al., 2011; Ahlm et al., 2013;
55 Hallar et al., 2013; Dzepina et al., 2015) and real-time measurements using online aerosol mass spectrometers (e.g.,
56 Zhang et al., 2007; Cozic et al., 2008; Sun et al., 2009; Fröhlich et al., 2015; Rinaldi et al., 2015; Freney et al.,
57 2016)(e.g., Zhang et al., 2007; Cozic et al., 2008; Sun et al., 2009; Fröhlich et al., 2015; Rinaldi et al., 2015; Freney
58 et al., 2016). These measurements have provided valuable information on the chemical and physical properties of
59 remote aerosols in the FT and PBL as well as how they are influenced by various sources (e.g., biomass burning, dust,
60 and biogenic emissions) and atmospheric processes (e.g., new particle formation, long-range transport, and cloud
61 processing).

62 The Mt. Bachelor Observatory (MBO) is a high-altitude atmospheric research site that has been utilized for
63 studying atmospheric chemistry in the western U.S. ~~for more than a decade~~ (Weiss-Penzias et al., 2006; Timonen et
64 al., 2013)(Weiss-Penzias et al., 2006; Timonen et al., 2013). The observatory is located at 2763 m above sea level at
65 the summit of Mt. Bachelor, a dormant volcano in the Deschutes National Forest in central Oregon (43.98° N, 121.69°
66 W). Due to its elevation, MBO is situated in the FT at night and is under the influence of upslope flow from the PBL
67 air during the daytime (McClure et al., 2016)(McClure et al., 2016). The remote characteristics of the site makes MBO
68 an ideal location for studying transported plumes, such as biomass burning plumes from regional and distant sources
69 (Jaffe et al., 2005b; Timonen et al., 2014; Briggs et al., 2016; Laing et al., 2016; Zhang and Jaffe, 2017; Zhang,

70 [2018](#)([Jaffe et al., 2005b](#); [Timonen et al., 2014](#); [Briggs et al., 2016](#); [Laing et al., 2016](#); [Zhang and Jaffe, 2017](#); [Zhang,](#)
71 [2018](#)) and long-range transport of Asian pollution in the spring ([Jaffe et al., 2005a](#); [Weiss-Penzias et al., 2006](#); [Fischer](#)
72 [et al., 2010](#); [Ambrose et al., 2011](#))([Jaffe et al., 2005a](#); [Weiss-Penzias et al., 2006](#); [Fischer et al., 2010](#); [Ambrose et al.,](#)
73 [2011](#)).

74 Continuous measurements of trace gases (e.g., ozone, carbon monoxide, carbon dioxide, mercury, nitrogen
75 oxides) and aerosol optical properties have been made at MBO since 2004. In summer 2013, a high-resolution time-
76 of-flight aerosol mass spectrometer (HR-AMS; Aerodyne Research, Inc.) was deployed at MBO as part of the US
77 Department of Energy sponsored Biomass Burning Observation Project (BBOP) ([Collier et al., 2016](#); [Zhou et al.,](#)
78 [2017](#))([Collier et al., 2016](#); [Zhou et al., 2017](#)). This was the first real-time, highly time-resolved aerosol chemical
79 measurement study performed at this site. ~~During this study,~~ MBO was frequently impacted by transported wildfire
80 plumes ~~during summer 2017~~ ([Collier et al., 2016](#); [Zhou et al., 2017](#))([Collier et al., 2016](#); [Zhou et al., 2017](#)) but ~~there~~
81 ~~were~~ during two periods, July 25 – 30 and August 17 – 21, ~~when~~ of this study the site was not influenced by wildfires
82 and the concentrations of air pollutants remained low. Here, we focus on [analyzing](#) these clean periods [in order](#) to
83 examine the chemical and physical properties of regional background aerosols and to investigate the differences of
84 aerosol characteristics and processes in the PBL and the FT over Western US.

85 2 Methods

86 The HR-AMS was deployed at MBO from July 25 to August 25, 2013, as part of the BBOP campaign. Ambient
87 aerosols were drawn through a PM_{2.5} cyclone inlet and dehumidified by a Nafion dryer to eliminate potential RH
88 effects on collection efficiency (CE). Treated particles then alternated between a heated thermodenuder (TD) line and
89 an ambient bypass line every 5 minutes before entering the HR-AMS. Aerosol scattering (TSI nephelometer; 1 μm
90 size cut), aerosol absorption (Tricolor Absorption Photometer, Brechtel; 1 μm size cut), CO and CO₂ (Picarro Cavity
91 Ring-Down Spectroscopy G2502), O₃ (Dasibi), NO_x (Air Quality Design 2-channel chemiluminescence), NO_y
92 (chemiluminescence), and peroxyacetyl nitrate (PAN; custom gas chromatograph) were also measured. Water vapor
93 mixing ratios were calculated from the measured temperature, relative humidity (Campbell Scientific HMP 45C) and
94 pressure (Vaisala PTB101B) following Bolton (1980), and typically agreed to within ± 15% and ± 0.3 g kg⁻¹ (Ambrose
95 et al., 2011). Additional details of the instrumentation and methodology can be found in previous publications (Briggs
96 et al., 2016; Collier et al., 2016; [Zhou et al., 2017](#)).

97 HR-AMS data were analyzed using [the](#) established data analysis software tool Squirrel (v1.53) and Pika (v1.12;
98 <http://cires1.colorado.edu/jimenez-group/ToFAMSResources/ToFSoftware>). A composition-dependent CE ~~was~~
99 ~~applied based on the algorithm by Middlebrook et al. (2012)~~ ([ranging from 0.5 to 1; average = 0.66](#)) ~~was applied based~~
100 ~~on the algorithm by Middlebrook et al. (2012)~~ to account for possible CE changes induced by changes in particle
101 phase in the AMS. A time-dependent gas phase CO₂⁺ subtraction (Collier and Zhang, 2013) was performed to improve
102 the quantification of organic aerosol (OA), which is critical for low aerosol loading conditions ([Setyan et al.,](#)
103 [2012](#))([Setyan et al., 2012](#)). Elemental analysis of high-resolution mass spectra (HRMS) utilized both the Aiken-
104 Ambient (AA) method (Aiken et al., 2008) and the Improved-Ambient (IA) method (Canagaratna et al., 2015).

Field Code Changed

105 Positive Matrix Factorization (PMF) was executed using the PMF2 algorithm (Paatero and Tapper,
106 1994)(Paatero and Tapper, 1994) in the PET v2.05 program (Ulbrich et al., 2009)(Ulbrich et al., 2009) on the
107 combined spectral matrices of organic and inorganic species (Sun et al., 2012; Zhou et al., 2017)(Sun et al., 2012;
108 Zhou et al., 2017) during the clean periods without wildfire impact (i.e., July 25 – 30 and August 17 – 21). Organic
109 ions at m/z 12 – 180 and major inorganic ions, i.e., SO^+ , SO_2^+ , HSO_2^+ , SO_3^+ , HSO_3^+ , and H_2SO_4^+ for sulfate, NO^+ and
110 NO_2^+ for nitrate, NH^+ , NH_2^+ , and NH_3^+ for ammonium, and HCl^+ for chloride were included. The error matrix was
111 pre-treated based on the procedures described in Ulbrich et al. (2009)Ulbrich et al. (2009). After PMF analysis, the
112 mass concentration of each OA factor was derived from the sum of organic signals in the corresponding mass spectrum
113 after applying the default relative ionization efficiency ($\text{RIE} = 1.4$) for organics and the time-dependent CE. The
114 solutions for 2 to 5 factors were explored with varying rotational parameters ($-0.5 \leq \text{FPEAK} \leq 0.5$, in increments of
115 0.1). Following the procedure listed in Table 1 in Zhang et al. (2011)Zhang et al. (2011), PMF solutions were evaluated
116 by investigating the key diagnostic plots, mass spectra, correlations with external tracers, and diurnal profiles. As
117 shown in Fig. S1 in the supplementary material, the 2-factor solution showed relatively large residual while the
118 4-factor solution showed signs of factor splitting. The 3-factor solution resolved a less oxidized oxygenated OA (OOA)
119 factor, a more oxidized OOA associated with some sulfate signals, and a sulfate-dominated OOA (Figs. S2 and S3).
120 As the sulfate-dominated OOA accounted for only 3% of the total organic signal and its O/C and HRMS highly
121 resembled those in the more-oxidized OOA factor (Fig. S3), these two factors were combined to form a so-called
122 “highly oxidized OOA” factor which has an O/C of 1.17. Based on the chemical, physical characteristics and the
123 volatility properties (see detailed discussions in Sect. 3.3), the less oxidized OOA was found to be semi-volatile OOA
124 (SV-OOA) mainly associated with fresher air masses from the BL whereas the highly oxidized OOA was comprised
125 of low-volatility organic compounds (LV-OOA) representing regional background OA in the FT. Furthermore, the
126 time series and mass spectra of the SV-OOA and LV-OOA derived here agreed well with the two background OOAs
127 derived from PMF analysis of the whole dataset, including the clean periods discussed in this study and the periods
128 influenced by wildfires (Zhou et al., 2017)(Zhou et al., 2017) (Figs. S4 and S5; $r^2 > 0.9$). This result suggests that the
129 PMF results for the clean periods are statistically significant and robust. All aerosol data in this analysis are reported
130 at ambient condition, except for aerosol light scattering, which is reported at STP ($T = 273\text{K}$ and $P = 1013.25\text{ hPa}$).

131 3 Results and Discussion

132 3.1. Temporal and Diurnal Variations of Regional Background Aerosols Observed at MBO

133 While observations at MBO were made continuously from July 25 to August 25, for this work, we use only data
134 from July 25 to 30 and August 17 to 21, 2013, which were relatively clear periods, free of wildfire influence. As
135 shown in Fig. 1, throughout the clean periods, classified as periods free of wildfire influence. The HR-AMS indicator for
136 biomass burning influence, namely the fraction of $\text{C}_2\text{H}_4\text{O}_2^+$ ($m/z = 60.021$) signal over total OA (f_{60}), was used for
137 differentiating wildfire influences. Periods with f_{60} below 0.3% (Fig. S6) likely received negligible influence from BB
138 (Cubison et al., 2011), thus were classified as clean periods. As shown in Fig. 1, throughout the clean periods, the CO
139 mixing ratio and submicron aerosol light scattering at 550 nm ($\sigma_{550\text{nm}}$) were below 120 ppb and 25 Mm^{-1} at STP,

140 respectively, similar to values previously observed at MBO under clean conditions (Fischer et al., 2011; Timonen et
141 al., 2014; Timonen et al., 2014). The site was influenced by transported wildfire plumes during the other periods of
142 BBOP and air pollutant levels increased substantially, e.g., CO and $\sigma_{550\text{nm}}$ increased by up to 8–10 times compared to
143 the clean periods and NR-PM₁ reached up to 140 $\mu\text{g m}^{-3}$ (Zhou et al., 2017)(Zhou et al., 2017). During the clean
144 periods, the HR-AMS indicator for biomass burning influence, namely the fraction of $\text{C}_2\text{H}_4\text{O}_2^+$ ($m/z = 60.021$) signal
145 over total OA (f_{60}), was below 0.3% (Fig. S6), confirming negligible influence from BB (Cubison et al., 2011).
146 Aerosol absorption data were available for the second clean period (August 17–21) and the average ($\pm 1\sigma$) EC mass
147 concentrations were estimated to be only 0.04 (± 0.14) $\mu\text{gC m}^{-3}$, further indicating a lack of BB influences.
148 Additionally, although winds at MBO showed a persistent westerly component (Fig. 1a and Fig. S7b), the bivariate
149 polar plot of NR-PM₁ concentrations exhibited a dispersed profile (Fig. S7c), indicating regional sources of aerosols
150 during the clean periods.

151 The average ($\pm 1\sigma$) concentration of NR-PM₁ (= sulfate + ammonium + nitrate + organics + chloride) during
152 these two clean periods was 2.8 (± 2.8) $\mu\text{g m}^{-3}$. OA was the largest PM₁ component, contributing on average ~84%
153 to the total NR-PM₁ mass, followed by sulfate (11%), ammonium (2.8%), and nitrate (0.9%), and chloride (0.1%)
154 (Fig. S7a). Chloride was close or below detection limit for most of the time during the clean periods. Aerosol
155 concentration and composition varied noticeably and showed diurnal changes that appeared to be mainly driven by
156 BL dynamics. This is because MBO sits in the FT at night but is influenced by air masses transported from the PBL
157 as the mixed layer height grows during the day. Indeed, the diurnal profile of the mixing-layer height retrieved from
158 the HYbrid Single Particle Lagrangian Integrated Trajectory (HYSPLIT) model (Draxler, 1998) shows that the MBO
159 is within the PBL between 12–8 pm PST (Fig. 2). In addition, previous studies at MBO have shown that water vapor
160 mixing ratio ($\text{H}_2\text{O}_{(\text{g})}$) can be used to differentiate BL-influenced and FT air masses as FT conditions tend to be very
161 dry (Weiss-Penzias et al., 2006; Reidmiller et al., 2010; McClure et al., 2016; Zhang and Jaffe, 2017)(Weiss-Penzias
162 et al., 2006; Reidmiller et al., 2010; McClure et al., 2016; Zhang and Jaffe, 2017). $\text{H}_2\text{O}_{(\text{g})}$ at MBO varied from as low
163 as 0.42 g kg^{-1} at night to as high as 6.9 g kg^{-1} during the day (Fig. 1b) and showed a strong diurnal cycle similar to
164 BLH boundary layer height (BLH) and NO_y/CO (Fig. 2), another parameter for differentiating BL-influenced and FT
165 air (Stohl et al., 2002)(Stohl et al., 2002).

166 NR-PM₁ and $\sigma_{550\text{nm}}$ generally followed the temporal trend of $\text{H}_2\text{O}_{(\text{g})}$ (Fig. 1b and c) and presented a pronounced
167 diurnal profile with substantial daytime enhancements (Fig. 2). The median mass concentration of NR-PM₁ was 0.5
168 $\mu\text{g m}^{-3}$ at night and increased by more than 10 times to 5.6 $\mu\text{g m}^{-3}$ in the afternoon. Similar temporal variations and
169 substantial daytime increases were observed for OA, nitrate, and gaseous pollutants such as CO, NO_y , and
170 peroxyacetyl nitrate (PAN) (Figs. 1 and 2), indicating that these species are primarily emitted or formed within the
171 BL and their concentrations at MBO are strongly influenced by BL dynamics. At night, the site is situated in the FT,
172 above the shallow nocturnal BL formed over the surrounding lower areas and disconnected from aerosol and gas
173 sources at the low altitudes. As the BL grows during the day, convective transport and thermal winds entrain pollution
174 from lower altitudes and increase air pollutants at the site. In contrast, sulfate and ammonium exhibited relatively
175 constant concentrations (Fig. 1e) and a less pronounced diurnal pattern (Fig. 2). The weaker influence from
176 BL evolution indicates similar sulfate and ammonium concentrations in the BL and in the FT in the remote continental

177 region of the western US—and, This is consistent with the relatively long atmospheric lifetime and the regional
178 characteristics of sulfate particles. O₃ and NO₂ mixing ratios also showed flat diurnal patterns (Fig. 2). However, a
179 previous study at MBO indicates that O₃ is typically higher in FT air masses (Zhang and Jaffe, 2017) but this depends
180 on the air mass origin and photochemical processing in both the BL and FT.

181 NR-PM₁ composition varied diurnally with a predominant organic composition during the day (up to 94% of
182 NR-PM₁ mass; Figs. 1 and 2). However, at night when the site was situated in the FT, sulfate was a major component
183 of aerosol (max = 83% of NR-PM₁; median = 37.6%; mean = 33%). OA during the clean periods at MBO was oxidized
184 with an average ($\pm 1\sigma$) O/C of 0.85 (± 0.36) and OM/OC of 2.26 (± 0.46). The degree of oxidation was in agreement
185 with regional background OA observed at other mountain sites such as Whistler Mountain in western Canada (Sun et
186 al., 2009)(Sun et al., 2009), Rocky Mountains in Colorado US (Schurman et al., 2015)(Schurman et al., 2015), and
187 Mt. Cimone in Italy (Rinaldi et al., 2015)(Rinaldi et al., 2015). In addition, OA observed under the FT condition was
188 overall more oxidized than those in the BL-influenced air masses. For example, O/C peaked at night with a maximum
189 value of 1.5 and reached a minimum of 0.7 in the afternoon (Fig. 2). H/C anti-correlated with O/C with a reversed
190 diurnal trend that peaked during daytime. As a result, the average oxidation state of carbon (OS_C; = 2 O/C – H/C;
191 (Krøll et al., 2011)(Krøll et al., 2011)) of OA at MBO during clean periods differs by 2 units between day and night
192 (Fig. 2). These trends highlight the different chemical properties as well as atmospheric ages of aerosols in the BL and
193 the FT in this remote continental region in the western US. More discussions on the differences between aerosols in
194 BL and FT air masses are given in Section 3.4.

195 3.2. Organonitrates and Organosulfates in Regional Background Aerosols

196 Particulate organonitrates have been shown to make a significant contribution to submicron aerosol mass,
197 especially in rural and remote environments during summertime (Setyan et al., 2012; Fry et al., 2013; Kiendler-Scharr
198 et al., 2016; Zhou et al., 2016)(Setyan et al., 2012; Fry et al., 2013; Kiendler-Scharr et al., 2016; Zhou et al., 2016). In
199 this study, organonitrates were observed and appeared to account for most of the NO⁺ and NO₂⁺ (major ions of
200 inorganic and organic nitrates in HR-AMS) signals detected in NR-PM₁ during the clean periods. This is because the
201 signal ratios of NO⁺ and NO₂⁺ measured for MBO aerosols, which ranged between 2.0 and 34.4 (average = 7.5; Fig.
202 S9a), are substantially higher compared to the ratio for pure ammonium nitrate particles (R_{AN} = 1.78 \pm 0.07). Previous
203 studies reported that the NO⁺/NO₂⁺ ratio for organonitrates (R_{ON}) are ~2.25 - 3.7 times higher than R_{AN} (Fry et al.,
204 2009; (Fry et al., 2009; Farmer et al., 2010; Fry et al., 2013); Fry et al., 2013). Based on this information and using
205 the equation (1) reported in Farmer et al. (2010), we estimated that nearly all the NO⁺ and NO₂⁺ signals measured
206 during the clean periods were contributed by organonitrates (RONO₂) from the fragmentation of the nitrate functional
207 group (-ONO₂). Assuming that organonitrate molecules on average contain one -ONO₂ functional group per molecule
208 and have an average molecular weight of 230 g mol⁻¹ (Lee et al., 2006; Fry et al., 2009)(Lee et al., 2006; Fry et al.,
209 2009), we estimated that the average concentration of organonitrates was 0.13 (\pm 0.12) μ g m⁻³ (Fig. S9b) and accounted
210 for ~5% of the total OA mass at MBO during the clean periods. Since MBO is situated in a forested region covered
211 by coniferous trees at lower elevations, the reactions of monoterpenes with nitrate radicals were likely an important
212 source of the observed particulate organonitrates (Fry et al., 2009; Fry et al., 2013; (Fry et al., 2009; Fry et al., 2013;

Field Code Changed

Boyd et al., 2015; Ng et al., 2017; Ng et al., 2017) in upslope daytime air. Similarly, Lee et al. (2016) observed that organonitrates made a significant contribution to the secondary OA (SOA) mass in the coniferous forested regions at Whistler – a mid-altitude site in western Canada.

The presence of organosulfur compounds in particles is also confirmed based on the unambiguous detection of sulfur-containing organic ions ($C_xH_yS_qO_z^+$) such as CH_3S^+ ($m/z = 46.996$), $CH_2SO_2^{+}$ ($m/z = 77.978$), $CH_3SO_2^{+}$ ($m/z = 78.985$), $CH_4SO_3^+$, CH_3S^+ ($m/z = 95.988$), $C_3H_3SO_2^{+}$ ($m/z = 105.001$), and $C_4H_3SO_2^{+}$ ($m/z = 117.001$). Previous studies have shown that $CH_2SO_2^+$, $CH_3SO_2^+$, and $CH_4SO_3^+$ are HR-AMS signature ions for methanesulfonic acid (MSA) (Ge et al., 2012)(Ge et al., 2012). In this study, the three ions correlate with each other ($r = 0.50 - 0.71$; Fig. S10) with their signal ratios are close to those observed for pure methanesulfonic acid (Ge et al., 2012)(Ge et al., 2012). This is an indication that indicates the presence of mesylate ($CH_3SO_3^-$, the deprotonated anion of MSA) was present in the regional background aerosols in the western US. Based on the fragmentation pattern of MSA, where $CH_3SO_2^+$ intensity contributed 8.7% of the total major MSA fragments in the HR-AMS spectrum of MSA (Ge et al., 2012)(Ge et al., 2012), we estimated that the average MSA mass concentration was $6.7 (\pm 7.2) \text{ ng m}^{-3}$, making up ~0.3% of the total OA mass during the clean periods.

we estimated that the average MSA mass concentration was $6.7 (\pm 7.2) \text{ ng m}^{-3}$, making up ~0.3% of the total OA mass during the clean periods. Sorooshian et al. (2015) measured MSA and organosulfates at inland ground sites near MBO and found broadly similar concentrations.

Oceans are generally considered a dominant source of dimethyl sulfide (DMS) and therefore its oxidation product MSA. However, the Pacific Ocean is 195 km to the west of MBO whereas the bivariate polar plot of MSA revealed that high concentrations were associated with winds from the east and the south (Fig. S11). This is an indication that the sources of MSA were mostly continental – the inland areas (Fig. S11). In addition, MSA concentrations showed a clear diurnal cycle with a substantial daytime increase (Fig. 2), which suggests significant sources from the PBL. Aerosols in the PBL over this region likely have negligible oceanic influences since the Cascades mountain range lies between the Pacific Ocean and Mt. Bachelor and may obstruct surface wind bringing marine emissions inland. DMS can be emitted from these results suggest that the sources of MSA at MBO were mostly continental, where a wide range of terrestrial sources including soil, vegetation, freshwater wetland, and paddy fields can emit DMS (Watts, 2000 and references therein)(Watts, 2000 and references therein). Furthermore, the maximum MSA/SO₄ ratio in this study was approximately 0.081, much lower than those observed in marine aerosols (e.g., average = 0.23 in sub-Arctic North East Pacific Ocean; (Phinney et al., 2006)(Phinney et al., 2006)). The Similarly, lower MSA/SO₄ ratios are much lower were usually found in terrestrial regions, e.g., 0.01 - 0.17 in Fresno where MSA was mostly attributed to non-marine sources (Ge et al., 2012; Young et al., 2016)(Ge et al., 2012; Young et al., 2016) and, 0.007 - 0.15 along the Atlantic coast under continental influences (Zorn et al., 2008; (Zorn et al., 2008; Huang et al., 2017), and averages of 0.02 - 0.04 (maximum = 0.11) in California inland regions (Sorooshian et al., 2015).

3.3. Sources and Processes of Aerosols in the Remote Region of the Western US

PMF analysis was performed on the NR-PM₁ mass spectra acquired during the clean periods to further elucidate the sources and processes of the regional background aerosols observed at MBO. Two OA factors were identified,

249 including an intermediately oxidized, semi-volatile OOA (SV-OOA, O/C = 0.67; H/C = 1.57) and a highly oxidized,
250 low volatility OOA (LV-OOA, O/C = 1.17 ± 0.08; H/C = 1.18 ± 0.03). No hydrocarbon-like (HOA) factor was
251 identified during the clean periods, which is consistent with a low abundance of C₄H₉⁺-signal (0.13% of total OA
252 signal), a tracer ion for primary OA from vehicle emissions (Collier et al., 2015). In addition, f₆₀ was constantly lower
253 than 0.3% (Fig. S6 and Fig. S13b), indicating a lack of BB influence (Cubison et al., 2011). These results indicate the
254 absence of primary aerosol sources at MBO during clean periods.

255 SV-OOA, which on average accounted for 70% of total OA mass at MBO during clean periods (Fig. 3c), showed
256 temporal features that indicate a strong influence from BL dynamics. Particularly, SV-OOA correlated well with CO,
257 nitrate, and MSA (r = 0.7 – 0.84) and exhibited a pronounced diurnal cycle that increases between 9:00 – 10:00, peaks
258 around 15:30 (PST), and decreases to a very low concentration (~ 0.1 µg m⁻³) at night (Fig. 2). The SV-OOA mass
259 spectrum displayed the characteristics of secondary OA (SOA) with two dominant oxygenated ions, C₂H₃O⁺ (m/z =
260 43.018) and CO₂⁺ (m/z = 43.989) (Fig. 3a). The signal intensity of C₂H₃O⁺ is similar to that of CO₂⁺ and the SV-OOA
261 spectrum comprises relatively abundant C_xH_y⁺ and C_xH_yO₁⁺ ions (Fig. 3a). These features, as well as an average O/C
262 of 0.67, indicate that SV-OOA was moderately oxidized and was likely not very aged.

263 The SV-OOA spectrum showed a significant C₇H₇⁺ signal (at m/z = 91.055), which (f_{C₇H₇⁺} = 0.65%) and a
264 spectral pattern highly similar to biogenic SOA observed from a plant chamber (Kiendler-Scharr et al., 2009). C₇H₇⁺
265 was proposed as an indicator for the presence of β-pinene + NO₃ reaction products (Boyd et al., 2015). Elevated C₂H₂⁺
266 is an and elevated f_{C₇H₇⁺} was previously observed in the AMS spectral feature for spectra of biogenic SOA observed
267 both in ambient air and in chamber experiments (Kiendler-Scharr et al., 2009; Sun et al., 2009; Robinson et al.,
268 2011; Setyan et al., 2012) (Kiendler-Scharr et al., 2009; Sun et al., 2009; Robinson et al., 2011; Setyan et al., 2012;
269 Budisulistiorini et al., 2015; Chen et al., 2015). In fact, addition, as shown in Fig. S13a, the SV-OOA spectrum of this
270 study is highly similar to situates along the spectrally right leg of biogenic SOA observed the triangle defined by
271 worldwide ambient OA in the f₄₄ vs f₄₃ space. It has been illustrated previously in both laboratory that the f₄₄ vs. f₄₃
272 triangle plot could be used to indicate the source/type of the aerosols and field studies that biogenic OA usually situate
273 on the right hand side of the triangle (Jimenez et al., 2009; Ng et al., 2010). These findings as well as, together with
274 the fact that organonitrates were predominantly associated with SV-OOA (Fig. e.g., 78% of the aerosol nitrate signal
275 was attributed to SV-OOA; Fig. S12), indicate that the SV-OOA observed in this study likely represented biogenic
276 SOA formed at lower altitudes in the region and transported upward to the site by thermal winds during the day.

277 LV-OOA, which accounted for an average 30% of total OA mass, likely represented more aged SOA in the
278 regional background air. It exhibited a much less pronounced diurnal trend than SV-OOA (Fig. 2) and presented as a
279 major OA component during most nights when the site was in the FT (Fig. 1g). These results suggest that LV-OOA
280 likely represents OA in the FT, which can be were transported over long-distance transported and/or regionally
281 recirculated regionally due to longer aerosol lifetime and higher wind speed in the FT. LV-OOA was highly oxidized
282 with an average O/C of 1.17 (Fig. 3b) and contributed major fractions of highly oxygenated organic ions, e.g.,
283 C₄H₃O₃⁺ (m/z = 99.008), C₃H₃O₃⁺ (m/z = 89.024), and C₆H₅O₃⁺ (m/z = 125.024), and CO₂⁺ and CHO₂⁺ (m/z =
284 44.998) – HR-AMS signature ions for carboxylic acids (Fig. 3e). In contrast, nearly all the C₈H₁₁⁺ (m/z = 107.086),
285 C₆H₁₁O⁺ (m/z = 99.081), C₅H₉⁺ (m/z = 69.070) and C₃H₇⁺ (m/z = 43.055) signals were attributed to SV-OOA, so were

Formatted: Font color: Black, German (Germany)

Formatted: Font color: Auto, English (United States)

Formatted: Not Superscript/ Subscript

286 a majority of the $C_4H_7^+$ ($m/z = 55.055$; 91%) and $C_2H_3O^+$ (86%) signals (Fig. 3d and 3e). In addition, LV-OOA was
287 tightly associated with sulfate (Fig. 3b and 3e), a secondary aerosol species representative of aged, regional air masses.
288 Furthermore, LV-OOA situates near the apex of the triangle region for ambient OAs in the f_{44} vs f_{43} space (Fig. S13a),
289 overlapping with the highly oxidized LV-OOA observed in various environments (Ng et al., 2010)(Ng et al., 2010) as
290 well as highly aged OOAs observed at high altitude (Sun et al., 2009; Fröhlich et al., 2015)(Sun et al., 2009; Fröhlich
291 et al., 2015). These results together suggest that LV-OOA likely represented free tropospheric SOA in the western
292 U.S and were composed of highly oxidized organic compounds.

293 3.4 Differences between Aerosols in BL and FT Air Masses

294 ~~Because MBO tends to sample the free troposphere air at night and the regional boundary layer air during the~~
295 ~~day, the measurement data are used to~~ To further examine the differences between aerosols in ~~both parts of the~~
296 ~~atmosphere during clean~~ the free troposphere and boundary layer, we segregate periods ~~using measurements of water~~
297 ~~vapor ($H_2O_{(g)}$).~~ Extensive work has been done to differentiate free tropospheric air from boundary layer-influenced air
298 at MBO using water vapor chairlift soundings (Reidmiller et al., 2010)(Reidmiller et al., 2010) and other approaches
299 (Weiss-Penzias et al., 2006)(Weiss-Penzias et al., 2006; Fischer et al., 2010; Ambrose et al., 2011; McClure et al.,
300 2016; Zhang and Jaffe, 2017)(McClure et al., 2016; Zhang and Jaffe, 2017). Zhang and Jaffe (2017) contributed to a
301 ~~more accurate monthly FT/BL influence isolation at MBO based on comparison of MBO $H_2O_{(g)}$ distributions to the~~
302 ~~$H_2O_{(g)}$ soundings from Medford and Salem, Oregon, at equivalent pressure level. Based on this work we classify~~
303 ~~periods with $H_2O_{(g)}$ above the minimum monthly water vapor criteria value, 2.5 g kg^{-1} , and $CO > 80 \text{ ppb}$ as those~~
304 ~~dominated by “BL-influenced air” and the rest by “FT air”. A discussion on the comparison between this method and~~
305 ~~using the estimated BL height as the differentiating criteria can be found in Section 1 of the Supplement.~~

306 The average concentration of NR- PM_{10} under BL influences was $3.16 \mu\text{g m}^{-3}$, approximately 4 times of that, as
307 discussed in more detail in Section 1 of the Supplement. Zhang and Jaffe (2017) established more accurate monthly
308 $H_2O_{(g)}$ criteria for FT air masses at MBO – 5.1 and 5.2 g kg^{-1} for July and August, respectively, and associated FT air
309 masses with low $H_2O_{(g)}$ values. However, since convection in summer enhances vertical transport and creates a thicker
310 entrainment zone where BL mixed with FT, properly defining the top of BL is challenging (Wagner et al., 2015). To
311 avoid the influences of the transition zone on FT, we used a more stringent $H_2O_{(g)}$ criterion, 2.5 g kg^{-1} , which is the
312 lowest monthly cut point reported in Zhang and Jaffe (2017). In addition, we explored the usage of the estimated BL
313 height from HYSPLIT back trajectory analysis as the segregation criteria. A comparison between these two methods
314 can be found in Section 1 of the Supplement. After careful evaluation, we classify periods with $H_2O_{(g)} < 2.5 \text{ g kg}^{-1}$ and
315 $CO < 80 \text{ ppb}$ as “FT air” and the rest as “BL-influenced air”.

316 The average concentration of NR- PM_{10} under BL influences was $3.16 \mu\text{g m}^{-3}$, approximately 4 times of the
317 average concentration in the FT ($0.85 \mu\text{g m}^{-3}$). While OA mass concentration was on average 6 times higher in the BL-
318 influenced air than in the FT air (2.7 vs $0.34 \mu\text{g m}^{-3}$), sulfate mass concentrations in these two types of air masses were
319 similar (0.35 vs $0.33 \mu\text{g m}^{-3}$). The stoichiometric neutralization of the inorganic components of NR- PM_{10} was examined
320 by comparing the molar equivalent ratio of ammonium ($[NH_4^+]/18$) and sulfate ($[SO_4^{2-}]/48$) since inorganic nitrate
321 and chloride concentrations appeared to be negligible were very low during clean periods. The ammonium-to-

322 sulfate equivalent ratios in aerosols during clean periods ratio of 1 suggests neutral particles whereas a ratio
323 significantly lower than 1 suggests acidic particles. This ratio varied between 0.005 – 1 for clean periods (Fig. 4a),
324 indicating that remote aerosols in the western US were frequently acidic in the summer. Most significant is that a
325 substantial amount of FT aerosols (~ 78% of FT the NR-PM₁ mass in FT air vs 16% of BL the NR-PM₁ mass in BL-
326 influenced air) exhibited an ammonium-to-sulfate equivalent ratio lower than 0.3 (Fig. 4a), indicating the
327 presence/prevalence of very acidic particles in the free troposphere. Acidic FT particles were also observed at various
328 high-altitude regional background sites, such as Jungfraujoch (Cozic et al., 2008; Fröhlich et al., 2015); Fröhlich et
329 al., 2015), Puy de Dome station (Freney et al., 2016), Whistler mountain (Sun et al., 2009)(Sun et al., 2009), and
330 Mauna Loa (Hawaii, US) (Johnson and Kumar, 1991)(Johnson and Kumar, 1991), and during airborne measurements
331 in the upper troposphere of the tropics (Froyd et al., 2009)(Froyd et al., 2009) and the Arctic (Brock et al., 2011; Fisher
332 et al., 2011).

333 MSA correlated with HR-AMS sulfate for different aerosol regimes with different slopes. As shown in Fig. 4b,
334 BL-influenced aerosols showed a range of MSA/SO₄ ratios generally higher than FT aerosols, possibly owing to
335 relatively abundant sulfate particles in the FT. When a polluted air mass is lifted out of the boundary layer, the already
336 formed aerosol can be washed out due to precipitation during lifting while the less soluble gas phase compounds such
337 as SO₂ are not entirely removed. The resulting gas phase mixture is then relatively enhanced in SO₂. Consequently,
338 during the subsequent regional transport in the FT, sulfate forms in larger concentrations than MSA. This may be
339 attributed to higher MSA concentration near terrestrial sources in the BL. Indeed, airborne measurements of MSA in
340 aerosol over the western US in summer 2013 have shown that MSA loading decreased with the increase of altitude
341 (Sorooshian et al., 2015). Furthermore, as discussed later on, sulfate was likely produced in the FT during regional
342 new particle formation and growth events, which may further contribute to lower MSA/SO₄ ratio in FT aerosols.

343 In addition to aerosol chemical properties, the physical properties of MBO aerosols were examined as well. The
344 average mass-based size distribution of NR-PM₁ during the clean periods displayed a broad feature extending from
345 100 to 1000 nm in vacuum aerodynamic diameter (D_{va}, Fig. 5). Aerosol composition varied as a function of size with
346 larger particles (>200 nm) having a relatively larger more enriched of sulfate contribution (12%) compared to than
347 smaller particles (<200 nm) (sulfate accounted for 12% of the non-refractory aerosol mass in PM_{>0.2} vs. 5% in PM_{<0.2}).
348 Org43, the organic signal at *m/z* = 43 (90% of which was C₂H₃O⁺), presented a broad distribution peaking between
349 250 and 350 nm in D_{va} (Fig. 5b). In contrast, Org44, the organic signal at *m/z* = 44 (95% of which was CO₂⁺), and
350 sulfate displayed distinctly narrower distributions peaking at a larger droplet accumulation mode close to 500 nm (Fig.
351 5b and 5c). The similar size distribution of Org44 and sulfate and the tight correlation between their concentrations
352 (*r*² = 0.61; Fig. S14) suggest that highly oxidized organics and sulfate had similar sources and processes and are
353 possibly internally mixed. In particular, the prominent droplet mode at 500 nm indicates an important influence of
354 aqueous-phase reactions on the production of sulfate and highly oxidized organics. Indeed, previous studies have
355 shown that aqueous-phase processing (i.e., fog and cloud droplets and aerosol phase water) have led/leads to production
356 of more oxidized organics (Lee et al., 2011; Lee et al., 2012; (Lee et al., 2011; Lee et al., 2012; Ervens et al., 2013);
357 Kim et al., 2019) in the droplet mode (Ge et al., 2012)(Ge et al., 2012) and that aqueous-phase production of sulfate

358 is an important process in the atmosphere (e.g., Ervens et al., 2011). In addition, a similar sulfate size distribution was
359 observed at the peak of Whistler Mountain, which had frequent cloud cover (Sun et al., 2009)(Sun et al., 2009).

360 A distinctly different size distribution was observed for sulfate-containing particles in the FT, ~~as shown in (Fig.~~
361 ~~5c, where it), which~~ exhibited a prominent mode at ~ 250 nm. One possible explanation is ~~econdensationalpreferential~~
362 ~~activation/wash out of larger particles, and thus the reduction of sulfate signal in larger size (droplet) modes.~~
363 ~~Condensational~~ growth of newly nucleated particles in the FT, ~~may be another possibility.~~ Scavenging ~~can~~
364 ~~significantly remove larger particles, resulting could result~~ in low particle surface area ~~that, which~~ facilitates new
365 particle formation (NPF) in the FT. ~~Indeed, Although we did not observe NPF events in this study (due to instrumental~~
366 ~~limitations),~~ in-situ NPF events have been frequently observed in the FT ~~at locations such as the Storm Peak~~
367 ~~Laboratory (Hallar et al., 2011; Hallar et al., 2013)(e.g., Hallar et al., 2011; Hallar et al., 2013), and Jungfraujoch~~
368 ~~(Bianchi et al., 2016; Tröstl et al., 2016), and in clean areas such as Aretie (Tunved et al., 2013; Freud et al., 2017).~~
369 ~~The formationFormation~~ and growth of new particles ~~has have~~ also been observed over ~~a broad regionregions~~ in the
370 FT (Tröstl et al., 2016)(Tröstl et al., 2016). ~~At MBO, daily thermal winds may have uplifted. Condensation of gas~~
371 ~~precursors from the BL to the phase sulfate products on small FT, which can be further oxidized in the FT and then~~
372 ~~condensed onto new particles, leading could contribute~~ to the ~~econdensational growth of observed condensation mode~~
373 ~~sulfate~~ particles (Bianchi et al., 2016)~~at MBO~~. These observations ~~may~~ shed light on the different sources and
374 processes of aerosols in the BL and FT and suggest that sulfate and organic aerosols were likely present in ~~variable~~
375 ~~mixtures (i.e., both internal and external mixtures) at MBO.~~

376 3.5. Comparisons with Aerosols Observed at Other High-altitude Locations

377 Figure 6 summarizes the average composition of NR-PM₁ measured using AMS or Aerosol Chemical Speciation
378 Monitors (ACSM) at various elevated regional background ground sites (Zhang et al., 2007; Sun et al., 2009; Freney
379 et al., 2011; Worton et al., 2011; Fröhlich et al., 2015; Rinaldi et al., 2015; Schurman et al., 2015; (Zhang et al., 2007;
380 Sun et al., 2009; Worton et al., 2011; Fröhlich et al., 2015; Rinaldi et al., 2015; Ripoll et al., 2015; Schurman et al.,
381 2015; Freney et al., 2016; Zhu et al., 2016; Xu et al., 2018); Zhu et al., 2016; Xu et al., 2018) and by aircraft (Bahreini
382 et al., 2003; Dunlea et al., 2009). All of these measurements were conducted under conditions absent of biomass
383 burning influence and ~~were~~ representative of regional background aerosols in the northern hemisphere. Mountain-top
384 studies separated FT air based on BLH calculated from LIDAR measurements (Freney et al., 2016) or tracers such as
385 ²²²Rn concentrations and NO_y/CO and back trajectory analysis (Fröhlich et al., 2015)(Fröhlich et al., 2015). The
386 average NR-PM₁ mass ~~econcentrations-concentration was 3.8 (± 3.4) µg m⁻³ across all sites was 5.1 (± 6.9) µg m⁻³ and~~
387 ~~the value in North America was 2.6 (± 1.6) µg m⁻³. in North America.~~ NR-PM₁ concentrations were, on average,
388 substantially lower in ~~the FT air~~ than in ~~the BL-influenced air~~ ($0.6889 \pm 0.4843 \mu\text{g m}^{-3}$ v.s. ~~5.8 ± 4.7; ± 3.4 µg m⁻³~~),
389 reflecting generally clean conditions in the FT.

390 A major fraction (27 – 84%; average = 51%) of the NR-PM₁ mass was organic matter at these remote high-
391 altitude locations (Fig. 6a). ~~Fe/OA in the FT air was generally more oxidized than that in the BL-influenced air (Fig.~~
392 ~~6b). In addition, for~~ the same site, marked chemical difference can be seen between aerosols in the FT and the BL. At
393 all sites, FT aerosols contained a substantially higher mass fraction of sulfate (39 – ~~4450~~%) compared to the mixed

394 BL/FT aerosols (11 – 35%). Aircraft measurements also showed consistent results of higher sulfate content in aerosols
395 at higher altitudes. For example, Bahreini et al. (2003) reported that the sulfate contribution to total NR-PM₁ over east
396 Asia increased from 17.4% in the lower atmosphere (1-3 km) to 28.8% in layers > 3 km. In the FT over the northeast
397 Pacific, more than half of the background submicron mass was attributed to sulfate (Dunlea et al., 2009; ~~Roberts et~~
398 ~~al., 2010~~Roberts et al., 2010). Elevated sulfate layers were also clearly observed in the higher altitudes above Mexico
399 City (DeCarlo et al., 2008). As a result, the mass ratio of submicron sulfate to organics (SO₄/Org) showed significantly
400 higher values (0.72 to 1.45) in the FT air masses than those in the mixed layers (0.13 – 0.7; Fig. 6b)

401 The extent to which sulfate particles are neutralized has major implications for aerosol radiative forcing. The
402 average relative humidity at MBO was 25.6 (±8.9) % during the clean periods. Acidic sulfate aerosols are more
403 hygroscopic than ammonium sulfate (Taylor et al., 2017), thus uptake of gaseous ammonia by acidic particles may
404 produce solid ammonium sulfate at low relative humidity. The resulting decrease in aerosol water content both
405 reduces the direct radiative forcing of sulfate (Adams et al., 2001) and increases the direct radiative forcing of sulfate (Adams
406 et al., 2001; Jacobson, 2001) and inhibits/promotes homogenous ice nucleation by liquid sulfate-
407 containing particles (Koop et al., 2000) (Koop et al., 2000). In addition, solid ammonium sulfate aerosols can also be
408 effective heterogeneous ice nuclei for cirrus cloud formation (Abbatt et al., 2006). While, In addition, while mineral
409 dust particles coated with ammonium sulfate are efficient ice nuclei, those coated with sulfuric acid can lose their
410 ice nucleating ability (Eastwood et al., 2009).

411 4. Summary and Conclusions

412 Based on field observations at a remote high-altitude atmospheric research station - the Mt. Bachelor Observatory
413 (MBO, 43.98° N, 121.69° W, 2763 m a.s.l.) in central Oregon - we have characterized the chemical and physical
414 properties of aerosols in the boundary layer and free troposphere air under clean conditions in the absence of wildfire
415 influences in the western US. Water vapor mixing ratio, a tracer used to segregate FT and BL-influenced air masses
416 at MBO, showed a strong diurnal cycle. Dry free tropospheric conditions were frequently observed at night, whereas
417 more humid, boundary layer influenced air was often observed at MBO during the day/daytime. The average (± 1σ)
418 NR-PM₁ mass concentration during the entire clean period was 2.8 (± 2.8) μg m⁻³, with OA dominating the NR-PM₁
419 composition (~ 84%) followed by sulfate (11%). OA, nitrate, and MSA displayed clear diurnal cycles with substantial
420 daytime increases, suggesting significantly higher mass concentrations in the BL than in the FT.

421 Strong diurnal patterns driven by the boundary layer dynamics were also observed in aerosol chemical
422 composition. NR-PM₁ contained a significantly higher mass fraction of sulfate (up to 83% of NR-PM₁ mass) and was
423 frequently acidic at night when MBO resided in the FT. In addition, nighttime free tropospheric OA was found to be
424 more oxidized. PMF analysis identified two types of OOA representing that are present in the regional background
425 OA air in the western US: a LV-OOA (30% of OA mass) that was highly oxidized (O/C = 1.17) and comprised of low-
426 volatility organics, representative of SOA in the free troposphere; and an SV-OOA (70% of OA mass) that was
427 intermediately oxidized (O/C = 0.67) and appeared to be semivolatile, representative of biogenic SOA originated in
428 the BL. In addition, the chemical compositions of NR-PM₁ observed at other high-altitude locations in the world under
429 regional background conditions were summarized. These results highlight the significant compositional major

430 differences between FT and BL aerosols, in that the FT aerosols are significantly more oxidized and contain a higher
431 fraction of sulfate. [These observations](#)[The observed compositional difference suggest significant differences between](#)
432 [FT and BL aerosols in microphysical and optical properties and](#) may have important implications for understanding
433 the climate effects of aerosols in remote regions.

434 **Data availability**

435 Data presented in this manuscript are available upon request to the corresponding author.

436 **Acknowledgements**

437 This ~~work is~~research was supported primarily by ~~US~~the U.S. Department of ~~Energy~~Energy's Atmospheric
438 System Research ~~Program~~, an Office of Science, Office of Biological and Environmental Research program, under
439 Grant No. DE-SC0014620. Shan Zhou [also](#) acknowledges funding from the Chinese Scholarship Council (CSC) and
440 the Donald G. Crosby Fellowship and the Fumio Matsumura Memorial Fellowship from the University of California
441 at Davis. The Mt. Bachelor Observatory is supported by the National Science Foundation (grant #AGS-1447832) and
442 the National Oceanic and Atmospheric Administration (contract #RA-133R-16-SE-0758).

443 **References**

444 [Abbatt, J. P. D., Benz, S., Cziezo, D. J., Kanji, Z., Lohmann, U., and Möhler, O.: Solid Ammonium Sulfate Aerosols](#)
445 [as Ice Nuclei: A Pathway for Cirrus Cloud Formation, Science, 313, 1770-1773, 2006.](#)

446 Adams, P. J., Seinfeld, J. H., Koch, D., Mickley, L., and Jacob, D.: General circulation model assessment of direct
447 radiative forcing by the sulfate-nitrate-ammonium-water inorganic aerosol system, *J. Geophys. Res. Atmos.*, 106,
448 1097-1111, 2001.

449 [Ahlm, L., Shakya, K. M., Russell, L. M., Schroder, J. C., Wong, J. P. S., Sjostedt, S. J., Hayden, K. L., Liggio, J.,](#)
450 [Wentzell, J. J. B., Wiebe, H. A., Mihele, C., Leaitch, W. R., and Macdonald, A. M.: Temperature-dependent](#)
451 [accumulation mode particle and cloud nuclei concentrations from biogenic sources during WACS 2010, Atmos.](#)
452 [Chem. Phys., 13, 3393-3407, 2013.](#)

453 Aiken, A. C., Decarlo, P. F., Kroll, J. H., Worsnop, D. R., Huffman, J. A., Docherty, K. S., Ulbrich, I. M., Mohr, C.,
454 Kimmel, J. R., Sueper, D., Sun, Y., Zhang, Q., Trimborn, A., Northway, M., Ziemann, P. J., Canagaratna, M. R.,
455 Onasch, T. B., Alfarra, M. R., Prevot, A. S. H., Dommen, J., Duplissy, J., Metzger, A., Baltensperger, U., and
456 Jimenez, J. L.: O/C and OM/OC ratios of primary, secondary, and ambient organic aerosols with high-resolution
457 time-of-flight aerosol mass spectrometry, *Environ. Sci. Tech.*, 42, 4478-4485, 2008.

458 Ambrose, J. L., Reidmiller, D. R., and Jaffe, D. A.: Causes of high O₃ in the lower free troposphere over the Pacific
459 Northwest as observed at the Mt. Bachelor Observatory, *Atmos. Environ.*, 45, 5302-5315, 2011.

460 Bahreini, R., Jimenez, J. L., Wang, J., Flagan, R. C., Seinfeld, J. H., Jayne, J. T., and Worsnop, D. R.: Aircraft-based
461 aerosol size and composition measurements during ACE-Asia using an Aerodyne aerosol mass spectrometer, *J.*
462 *Geophys. Res. Atmos.*, 108, 8645, 2003.

463 Bianchi, F., Trostl, J., Junninen, H., Frege, C., Henne, S., Hoyle, C. R., Molteni, U., Herrmann, E., Adamov, A.,
464 Bukowiecki, N., Chen, X., Duplissy, J., Gysel, M., Hutterli, M., Kangasluoma, J., Kontkanen, J., Kurten, A.,
465 Manninen, H. E., Munch, S., Perakyla, O., Petaja, T., Rondo, L., Williamson, C., Weingartner, E., Curtius, J.,
466 Worsnop, D. R., Kulmala, M., Dommen, J., and Baltensperger, U.: New particle formation in the free troposphere:
467 A question of chemistry and timing, *Science*, 352, 1109-1112, 2016.

468 Bolton, D.: The Computation of Equivalent Potential Temperature, *Monthly Weather Review*, 108, 1046-1053,
469 1980.

470 Boucher, O., D. Randall, P. Artaxo, C. Bretherton, G. Feingold, P. Forster, V.-M. Kerminen, Y. Kondo, H. Liao, U.
471 Lohmann, P. Rasch, S.K. Satheesh, S. Sherwood, B. Stevens and X.Y. Zhang: Clouds and Aerosols. In: *Climate*
472 *Change 2013: The Physical Science Basis. Contribution of Working Group I to the Fifth Assessment Report of the*
473 *Intergovernmental Panel on Climate Change*, Cambridge University Press, Cambridge, United Kingdom and New
474 York, NY, USA., 2013.

475 Boyd, C. M., Sanchez, J., Xu, L., Eugene, A. J., Nah, T., Tuet, W. Y., Guzman, M. I., and Ng, N. L.: Secondary
476 organic aerosol formation from the β -pinene+NO₃ system: effect of humidity and peroxy radical fate, *Atmos.*
477 *Chem. Phys.*, 15, 7497-7522, 2015.

478 Briggs, N. L., Jaffe, D. A., Gao, H., Hee, J. R., Baylon, P. M., Zhang, Q., Zhou, S., Collier, S. C., Sampson, P. D.,
479 and Cary, R. A.: Particulate Matter, Ozone, and Nitrogen Species in Aged Wildfire Plumes Observed at the Mount
480 Bachelor Observatory, *Aerosol Air Qual. Res.*, 16, 3075-3087, 2016.

481 Brock, C. A., Cozic, J., Bahreini, R., Froyd, K. D., Middlebrook, A. M., McComiskey, A., Brioude, J., Cooper, O.
482 R., Stohl, A., Aikin, K. C., de Gouw, J. A., Fahey, D. W., Ferrare, R. A., Gao, R. S., Gore, W., Holloway, J. S.,
483 Hübner, G., Jefferson, A., Lack, D. A., Lance, S., Moore, R. H., Murphy, D. M., Nenes, A., Novelli, P. C., Nowak, J.
484 B., Ogren, J. A., Peischl, J., Pierce, R. B., Pilewskie, P., Quinn, P. K., Ryerson, T. B., Schmidt, K. S., Schwarz, J. P.,
485 Sodemann, H., Spackman, J. R., Stark, H., Thomson, D. S., Thornberry, T., Veres, P., Watts, L. A., Warneke, C.,
486 and Wollny, A. G.: Characteristics, sources, and transport of aerosols measured in spring 2008 during the aerosol,
487 radiation, and cloud processes affecting Arctic Climate (ARCPAC) Project, *Atmos. Chem. Phys.*, 11, 2423-2453,
488 2011.

489 Budisulistiorini, S. H., Li, X., Bairai, S. T., Renfro, J., Liu, Y., Liu, Y. J., McKinney, K. A., Martin, S. T., McNeill,
490 V. F., Pye, H. O. T., Nenes, A., Neff, M. E., Stone, E. A., Mueller, S., Knote, C., Shaw, S. L., Zhang, Z., Gold, A.,
491 and Surratt, J. D.: Examining the effects of anthropogenic emissions on isoprene-derived secondary organic aerosol
492 formation during the 2013 Southern Oxidant and Aerosol Study (SOAS) at the Look Rock, Tennessee ground site,
493 *Atmos. Chem. Phys.*, 15, 8871-8888, 2015.

494 Canagaratna, M. R., Jimenez, J. L., Kroll, J. H., Chen, Q., Kessler, S. H., Massoli, P., Hildebrandt Ruiz, L., Fortner,
495 E., Williams, L. R., Wilson, K. R., Surratt, J. D., Donahue, N. M., Jayne, J. T., and Worsnop, D. R.: Elemental ratio
496 measurements of organic compounds using aerosol mass spectrometry: characterization, improved calibration, and
497 implications, *Atmos. Chem. Phys.*, 15, 253-272, 2015.

498 Chen, Q., Farmer, D. K., Rizzo, L. V., Pauliquevis, T., Kuwata, M., Karl, T. G., Guenther, A., Allan, J. D., Coe, H.,
499 Andreae, M. O., Pöschl, U., Jimenez, J. L., Artaxo, P., and Martin, S. T.: Submicron particle mass concentrations
500 and sources in the Amazonian wet season (AMAZE-08), *Atmos. Chem. Phys.*, 15, 3687-3701, 2015.

501 Collier, S. and Zhang, Q.: Gas-Phase CO₂ Subtraction for Improved Measurements of the Organic Aerosol Mass
502 Concentration and Oxidation Degree by an Aerosol Mass Spectrometer, *Environ. Sci. Tech.*, 47, 14324-14331,
503 2013.

504 Collier, S., Zhou, S., Kuwayama, T., Forestieri, S., Brady, J., Zhang, M., Kleeman, M., Cappa, C., Bertram, T., and
505 Zhang, Q.: Organic PM Emissions from Vehicles: Composition, O/C Ratio, and Dependence on PM Concentration,
506 *Aerosol Sci. Tech.*, 49, 86-97, 2015.

507 Collier, S., Zhou, S., Onasch, T. B., Jaffe, D. A., Kleinman, L., Sedlacek, A. J., Briggs, N. L., Hee, J., Fortner, E.,
508 Shilling, J. E., Worsnop, D., Yokelson, R. J., Parworth, C., Ge, X., Xu, J., Butterfield, Z., Chand, D., Dubey, M. K.,
509 Pekour, M. S., Springston, S., and Zhang, Q.: Regional Influence of Aerosol Emissions from Wildfires Driven by
510 Combustion Efficiency: Insights from the BBOP Campaign, *Environ. Sci. Tech.*, 50, 8613-8622, 2016.

511 Cozic, J., Verheggen, B., Weingartner, E., Crosier, J., Bower, K. N., Flynn, M., Coe, H., Henning, S., Steinbacher,
512 M., Henne, S., Collaud Coen, M., Petzold, A., and Baltensperger, U.: Chemical composition of free tropospheric
513 aerosol for PM₁ and coarse mode at the high alpine site Jungfraujoch, *Atmos. Chem. Phys.*, 8, 407-423, 2008.

514 Cubison, M. J., Ortega, A. M., Hayes, P. L., Farmer, D. K., Day, D., Lechner, M. J., Brune, W. H., Apel, E., Diskin,
515 G. S., Fisher, J. A., Fuelberg, H. E., Hecobian, A., Knapp, D. J., Mikoviny, T., Riemer, D., Sachse, G. W., Sessions,
516 W., Weber, R. J., Weinheimer, A. J., Wisthaler, A., and Jimenez, J. L.: Effects of aging on organic aerosol from
517 open biomass burning smoke in aircraft and laboratory studies, *Atmos. Chem. Phys.*, 11, 12049-12064, 2011.

518 DeCarlo, P. F., Dunlea, E. J., Kimmel, J. R., Aiken, A. C., Sueper, D., Crouse, J., Wennberg, P. O., Emmons, L.,
519 Shinzuka, Y., Clarke, A., Zhou, J., Tomlinson, J., Collins, D. R., Knapp, D., Weinheimer, A. J., Montzka, D. D.,
520 Campos, T., and Jimenez, J. L.: Fast airborne aerosol size and chemistry measurements above Mexico City and
521 Central Mexico during the MILAGRO campaign, *Atmos. Chem. Phys.*, 8, 4027-4048, 2008.

522 Draxler, R. R., Hess, G. D. : An overview of the Hysplit-4 modeling system for trajectories, dispersion, and
523 deposition, *Aust. Meteorol. Magn.* , 47, 295-308, 1998.

524 Dunlea, E. J., DeCarlo, P. F., Aiken, A. C., Kimmel, J. R., Peltier, R. E., Weber, R. J., Tomlinson, J., Collins, D. R.,
525 Shinzuka, Y., McNaughton, C. S., Howell, S. G., Clarke, A. D., Emmons, L. K., Apel, E. C., Pfister, G. G., van
526 Donkelaar, A., Martin, R. V., Millet, D. B., Heald, C. L., and Jimenez, J. L.: Evolution of Asian aerosols during
527 transpacific transport in INTEX-B, *Atmos. Chem. Phys.*, 9, 7257-7287, 2009.

528 Dzepina, K., Mazzoleni, C., Fialho, P., China, S., Zhang, B., Owen, R. C., Helmig, D., Hueber, J., Kumar, S.,
529 Perlinger, J. A., Kramer, L. J., Dziobak, M. P., Ampadu, M. T., Olsen, S., Wuebbles, D. J., and Mazzoleni, L. R.:
530 Molecular characterization of free tropospheric aerosol collected at the Pico Mountain Observatory: a case study
531 with a long-range transported biomass burning plume, *Atmos. Chem. Phys.*, 15, 5047-5068, 2015.

532 Eastwood, M. L., Cremel, S., Wheeler, M., Murray, B. J., Girard, E., and Bertram, A. K.: Effects of sulfuric acid and
533 ammonium sulfate coatings on the ice nucleation properties of kaolinite particles, *Geophys Res Lett*, 36, L02811,
534 2009.

535 Ervens, B., Turpin, B. J., and Weber, R. J.: Secondary organic aerosol formation in cloud droplets and aqueous
536 particles (aqSOA): a review of laboratory, field and model studies, *Atmos. Chem. Phys.*, 11, 11069-11102, 2011.

537 Ervens, B., Wang, Y., Eagar, J., Leaitch, W. R., Macdonald, A. M., Valsaraj, K. T., and Herckes, P.: Dissolved
538 organic carbon (DOC) and select aldehydes in cloud and fog water: the role of the aqueous phase in impacting trace
539 gas budgets, *Atmos. Chem. Phys.*, 13, 5117-5135, 2013.

- 540 Farmer, D. K., Matsunaga, A., Docherty, K. S., Surratt, J. D., Seinfeld, J. H., Ziemann, P. J., and Jimenez, J. L.:
541 Response of an aerosol mass spectrometer to organonitrates and organosulfates and implications for atmospheric
542 chemistry, *P. Natl. Acad. Sci. USA*, 107, 6670-6675, 2010.
- 543 Fischer, E. V., Jaffe, D. A., Reidmiller, D. R., and Jaegle, L.: Meteorological controls on observed peroxyacetyl
544 nitrate at Mount Bachelor during the spring of 2008, *J. Geophys. Res. Atmos.*, 115, 2010.
- 545 Fischer, E. V., Jaffe, D. A., and Weatherhead, E. C.: Free tropospheric peroxyacetyl nitrate (PAN) and ozone at
546 Mount Bachelor: potential causes of variability and timescale for trend detection, *Atmos. Chem. Phys.*, 11, 5641-
547 5654, 2011.
- 548 Fisher, J. A., Jacob, D. J., Wang, Q., Bahreini, R., Carouge, C. C., Cubison, M. J., Dibb, J. E., Diehl, T., Jimenez, J.
549 L., Leibensperger, E. M., Lu, Z., Meinders, M. B. J., Pye, H. O. T., Quinn, P. K., Sharma, S., Streets, D. G., van
550 Donkelaar, A., and Yantosca, R. M.: Sources, distribution, and acidity of sulfate-ammonium aerosol in the Arctic in
551 winter-spring, *Atmos. Environ.*, 45, 7301-7318, 2011.
- 552 Freney, E., Sellegri, K., Asmi, E., Rose, C., Chauvigne, A., Baray, J. L., Colomb, A., Hervo, M., Montoux, N.,
553 Bouvier, L., and Picard, D.: Experimental Evidence of the Feeding of the Free Troposphere with Aerosol Particles
554 from the Mixing Layer, *Aerosol Air Qual. Res.*, 16, 702-716, 2016.
- 555 Freney, E. J., Sellegri, K., Canonaco, F., Boulon, J., Hervo, M., Weigel, R., Pichon, J. M., Colomb, A., Prévôt, A. S.
556 H., and Laj, P.: Seasonal variations in aerosol particle composition at the puy-de-Dôme research station in France,
557 *Atmos. Chem. Phys.*, 11, 13047-13059, 2011.
- 558 [Freud, E., Krejci, R., Tunved, P., Leaitch, R., Nguyen, Q. T., Massling, A., Skov, H., and Barrie, L.: Pan-Arctic
559 aerosol number size distributions: seasonality and transport patterns, *Atmos. Chem. Phys.*, 17, 8101-8128, 2017.](#)
- 560 Fröhlich, R., Cubison, M. J., Slowik, J. G., Bukowiecki, N., Canonaco, F., Croteau, P. L., Gysel, M., Henne, S.,
561 Herrmann, E., Jayne, J. T., Steinbacher, M., Worsnop, D. R., Baltensperger, U., and Prévôt, A. S. H.: Fourteen
562 months of on-line measurements of the non-refractory submicron aerosol at the Jungfraujoch (3580 m a.s.l.) –
563 chemical composition, origins and organic aerosol sources, *Atmos. Chem. Phys.*, 15, 11373-11398, 2015.
- 564 Froyd, K. D., Murphy, D. M., Sanford, T. J., Thomson, D. S., Wilson, J. C., Pfister, L., and Lait, L.: Aerosol
565 composition of the tropical upper troposphere, *Atmos. Chem. Phys.*, 9, 4363-4385, 2009.
- 566 Fry, J. L., Draper, D. C., Zarzana, K. J., Campuzano-Jost, P., Day, D. A., Jimenez, J. L., Brown, S. S., Cohen, R. C.,
567 Kaser, L., Hansel, A., Cappellin, L., Karl, T., Roux, A. H., Turnipseed, A., Cantrell, C., Lefer, B. L., and Grossberg,
568 N.: Observations of gas- and aerosol-phase organic nitrates at BEACHON-RoMBAS 2011, *Atmos. Chem. Phys.*, 13,
569 8585-8605, 2013.
- 570 Fry, J. L., Kiendler-Scharr, A., Rollins, A. W., Wooldridge, P. J., Brown, S. S., Fuchs, H., Dube, W., Mensah, A.,
571 dal Maso, M., Tillmann, R., Dorn, H. P., Brauers, T., and Cohen, R. C.: Organic nitrate and secondary organic
572 aerosol yield from NO₃ oxidation of beta-pinene evaluated using a gas-phase kinetics/aerosol partitioning model,
573 *Atmos. Chem. Phys.*, 9, 1431-1449, 2009.
- 574 Ge, X. L., Zhang, Q., Sun, Y. L., Ruehl, C. R., and Setyan, A.: Effect of aqueous-phase processing on aerosol
575 chemistry and size distributions in Fresno, California, during wintertime, *Environ. Chem.*, 9, 221-235, 2012.

576 Hallar, A. G., Lowenthal, D. H., Chirokova, G., Borys, R. D., and Wiedinmyer, C.: Persistent daily new particle
577 formation at a mountain-top location, *Atmos. Environ.*, 45, 4111-4115, 2011.

578 Hallar, A. G., Lowenthal, D. H., Clegg, S. L., Samburova, V., Taylor, N., Mazzoleni, L. R., Zielinska, B. K.,
579 Kristensen, T. B., Chirokova, G., McCubbin, I. B., Dodson, C., and Collins, D.: Chemical and hygroscopic
580 properties of aerosol organics at Storm Peak Laboratory, *J. Geophys. Res. Atmos.*, 118, 4767-4779, 2013.

581 Hallar, A. G., Petersen, R., McCubbin, I. B., Lowenthal, D., Lee, S., Andrews, E., and Yu, F.: Climatology of New
582 Particle Formation and Corresponding Precursors at Storm Peak Laboratory, *Aerosol Air Qual. Res.*, 16, 816-826,
583 2016.

584 Huang, S., Poulain, L., van Pinxteren, D., van Pinxteren, M., Wu, Z., Herrmann, H., and Wiedensohler, A.:
585 Latitudinal and Seasonal Distribution of Particulate MSA over the Atlantic using a Validated Quantification Method
586 with HR-ToF-AMS, *Environ. Sci. Tech.*, 51, 418-426, 2017.

587 Jacobson, M. Z.: Global direct radiative forcing due to multicomponent anthropogenic and natural aerosols, *J.*
588 *Geophys. Res. Atmos.*, 106, 1551-1568, 2001.

589 Jaffe, D., Prestbo, E., Swartzendruber, P., Weiss-Penzias, P., Kato, S., Takami, A., Hatakeyama, S., and Kajii, Y.:
590 Export of atmospheric mercury from Asia, *Atmos. Environ.*, 39, 3029-3038, 2005a.

591 Jaffe, D., Tamura, S., and Harris, J.: Seasonal cycle and composition of background fine particles along the west
592 coast of the US, *Atmos. Environ.*, 39, 297-306, 2005b.

593 [Jimenez, J. L., Canagaratna, M. R., Donahue, N. M., Prevot, A. S. H., Zhang, Q., Kroll, J. H., DeCarlo, P. F., Allan,](#)
594 [J. D., Coe, H., Ng, N. L., Aiken, A. C., Docherty, K. S., Ulbrich, I. M., Grieshop, A. P., Robinson, A. L., Duplissy,](#)
595 [J., Smith, J. D., Wilson, K. R., Lanz, V. A., Hueglin, C., Sun, Y. L., Tian, J., Laaksonen, A., Raatikainen, T.,](#)
596 [Rautiainen, J., Vaattovaara, P., Ehn, M., Kulmala, M., Tomlinson, J. M., Collins, D. R., Cubison, M. J., Dunlea, E.](#)
597 [J., Huffman, J. A., Onasch, T. B., Alfarra, M. R., Williams, P. I., Bower, K., Kondo, Y., Schneider, J., Drewnick, F.,](#)
598 [Borrmann, S., Weimer, S., Demerjian, K., Salcedo, D., Cottrell, L., Griffin, R., Takami, A., Miyoshi, T.,](#)
599 [Hatakeyama, S., Shimono, A., Sun, J. Y., Zhang, Y. M., Dzepina, K., Kimmel, J. R., Sueper, D., Jayne, J. T.,](#)
600 [Herndon, S. C., Trimborn, A. M., Williams, L. R., Wood, E. C., Middlebrook, A. M., Kolb, C. E., Baltensperger, U.,](#)
601 [and Worsnop, D. R.: Evolution of Organic Aerosols in the Atmosphere, *Science*, 326, 1525-1529, 2009.](#)

602 Johnson, S. A. and Kumar, R.: Composition and spectral characteristics of ambient aerosol at Mauna Loa
603 Observatory, *J. Geophys. Res. Atmos.*, 96, 5379-5386, 1991.

604 Kiendler-Scharr, A., Mensah, A. A., Friese, E., Topping, D., Nemitz, E., Prevot, A. S. H., Aijala, M., Allan, J.,
605 Canonaco, F., Canagaratna, M., Carbone, S., Crippa, M., Dall'Osto, M., Day, D. A., De Carlo, P., Di Marco, C. F.,
606 Elbern, H., Eriksson, A., Freney, E., Hao, L., Herrmann, H., Hildebrandt, L., Hillamo, R., Jimenez, J. L., Laaksonen,
607 A., McFiggans, G., Mohr, C., O'Dowd, C., Otjes, R., Ovadnevaite, J., Pandis, S. N., Poulain, L., Schlag, P., Sellegri,
608 K., Swietlicki, E., Tiitta, P., Vermeulen, A., Wahner, A., Worsnop, D., and Wu, H. C.: Ubiquity of organic nitrates
609 from nighttime chemistry in the European submicron aerosol, *Geophys Res Lett*, 43, 7735-7744, 2016.

610 Kiendler-Scharr, A., Zhang, Q., Hohaus, T., Kleist, E., Mensah, A., Mentel, T. F., Spindler, C., Uerlings, R.,
611 Tillmann, R., and Wildt, J.: Aerosol Mass Spectrometric Features of Biogenic SOA: Observations from a Plant
612 Chamber and in Rural Atmospheric Environments, *Environ. Sci. Tech.*, 43, 8166-8172, 2009.

613 [Kim, H., Collier, S., Ge, X., Xu, J., Sun, Y., Jiang, W., Wang, Y., Herckes, P., and Zhang, Q.: Chemical processing](#)
614 [of water-soluble species and formation of secondary organic aerosol in fogs, *Atmos. Environ.*, 200, 158-166, 2019.](#)

615 Koop, T., Luo, B., Tsias, A., and Peter, T.: Water activity as the determinant for homogeneous ice nucleation in
616 aqueous solutions, *Nature*, 406, 611-614, 2000.

617 Kroll, J. H., Donahue, N. M., Jimenez, J. L., Kessler, S. H., Canagaratna, M. R., Wilson, K. R., Altieri, K. E.,
618 Mazzoleni, L. R., Wozniak, A. S., Bluhm, H., Mysak, E. R., Smith, J. D., Kolb, C. E., and Worsnop, D. R.: Carbon
619 oxidation state as a metric for describing the chemistry of atmospheric organic aerosol, *Nature Chemistry*, 3, 133-
620 139, 2011.

621 Laing, J. R., Jaffe, D. A., and Hee, J. R.: Physical and optical properties of aged biomass burning aerosol from
622 wildfires in Siberia and the Western USA at the Mt. Bachelor Observatory, *Atmos. Chem. Phys.*, 16, 15185-15197,
623 2016.

624 Lee, A., Goldstein, A. H., Keywood, M. D., Gao, S., Varutbangkul, V., Bahreini, R., Ng, N. L., Flagan, R. C., and
625 Seinfeld, J. H.: Gas-phase products and secondary aerosol yields from the ozonolysis of ten different terpenes, *J.*
626 *Geophys. Res. Atmos.*, 111, D07302, 2006.

627 Lee, A. K. Y., [Abbatt, J. P. D., Leaitch, W. R., Li, S. M., Sjostedt, S. J., Wentzell, J. J. B., Liggio, J., and](#)
628 [Macdonald, A. M.: Substantial secondary organic aerosol formation in a coniferous forest: observations of both day-](#)
629 [and nighttime chemistry, *Atmos. Chem. Phys.*, 16, 6721-6733, 2016.](#)

630 [Lee, A. K. Y.,](#) Hayden, K. L., Herckes, P., Leaitch, W. R., Liggio, J., Macdonald, A. M., and Abbatt, J. P. D.:
631 Characterization of aerosol and cloud water at a mountain site during WACS 2010: secondary organic aerosol
632 formation through oxidative cloud processing, *Atmos. Chem. Phys.*, 12, 7103-7116, 2012.

633 Lee, A. K. Y., Herckes, P., Leaitch, W. R., Macdonald, A. M., and Abbatt, J. P. D.: Aqueous OH oxidation of
634 ambient organic aerosol and cloud water organics: Formation of highly oxidized products, *Geophys Res Lett*, 38,
635 L11805, 2011.

636 McClure, C. D., Jaffe, D. A., and Gao, H.: Carbon Dioxide in the Free Troposphere and Boundary Layer at the Mt.
637 Bachelor Observatory, *Aerosol Air Qual. Res.*, 16, 717-728, 2016.

638 Middlebrook, A. M., Bahreini, R., Jimenez, J. L., and Canagaratna, M. R.: Evaluation of Composition-Dependent
639 Collection Efficiencies for the Aerodyne Aerosol Mass Spectrometer using Field Data, *Aerosol Sci. Tech.*, 46, 258-
640 271, 2012.

641 Ng, N. L., Brown, S. S., Archibald, A. T., Atlas, E., Cohen, R. C., Crowley, J. N., Day, D. A., Donahue, N. M., Fry,
642 J. L., Fuchs, H., Griffin, R. J., Guzman, M. I., Herrmann, H., Hodzic, A., Iinuma, Y., Jimenez, J. L., Kiendler-
643 Scharr, A., Lee, B. H., Luecken, D. J., Mao, J., McLaren, R., Mutzel, A., Osthoff, H. D., Ouyang, B., Picquet-
644 Varrault, B., Platt, U., Pye, H. O. T., Rudich, Y., Schwantes, R. H., Shiraiwa, M., Stutz, J., Thornton, J. A., Tilgner,
645 A., Williams, B. J., and Zaveri, R. A.: Nitrate radicals and biogenic volatile organic compounds: oxidation,
646 mechanisms, and organic aerosol, *Atmos. Chem. Phys.*, 17, 2103-2162, 2017.

647 Ng, N. L., Canagaratna, M. R., Zhang, Q., Jimenez, J. L., Tian, J., Ulbrich, I. M., Kroll, J. H., Docherty, K. S.,
648 Chhabra, P. S., Bahreini, R., Murphy, S. M., Seinfeld, J. H., Hildebrandt, L., Donahue, N. M., DeCarlo, P. F., Lanz,
649 V. A., Prevot, A. S. H., Dinar, E., Rudich, Y., and Worsnop, D. R.: Organic aerosol components observed in
650 Northern Hemispheric datasets from Aerosol Mass Spectrometry, *Atmos. Chem. Phys.*, 10, 4625-4641, 2010.

651 Paatero, P. and Tapper, U.: Positive Matrix Factorization - a Nonnegative Factor Model with Optimal Utilization of
652 Error-Estimates of Data Values, *Environmetrics*, 5, 111-126, 1994.

653 Phinney, L., Richard Leaitch, W., Lohmann, U., Boudries, H., Worsnop, D. R., Jayne, J. T., Toom-Sauntry, D.,
654 Wadleigh, M., Sharma, S., and Shantz, N.: Characterization of the aerosol over the sub-arctic north east Pacific
655 Ocean, *Deep Sea Res. II: Top. Stud. Oceanogr.*, 53, 2410-2433, 2006.

656 Reidmiller, D. R., Jaffe, D. A., Fischer, E. V., and Finley, B.: Nitrogen oxides in the boundary layer and free
657 troposphere at the Mt. Bachelor Observatory, *Atmos. Chem. Phys.*, 10, 6043-6062, 2010.

658 Rinaldi, M., Gilardoni, S., Paglione, M., Sandrini, S., Fuzzi, S., Massoli, P., Bonasoni, P., Cristofanelli, P.,
659 Marinoni, A., Poluzzi, V., and Decesari, S.: Organic aerosol evolution and transport observed at Mt. Cimone (2165
660 m a.s.l.), Italy, during the PEGASOS campaign, *Atmos. Chem. Phys.*, 15, 11327-11340, 2015.

661 [Ripoll, A., Minguillón, M. C., Pey, J., Jimenez, J. L., Day, D. A., Sosedova, Y., Canonaco, F., Prévôt, A. S. H.,](#)
662 [Querol, X., and Alastuey, A.: Long-term real-time chemical characterization of submicron aerosols at Montsec](#)
663 [\(southern Pyrenees, 1570 m a.s.l.\), *Atmos. Chem. Phys.*, 15, 2935-2951, 2015.](#)

664 Roberts, G. C., Day, D. A., Russell, L. M., Dunlea, E. J., Jimenez, J. L., Tomlinson, J. M., Collins, D. R.,
665 Shinzuka, Y., and Clarke, A. D.: Characterization of particle cloud droplet activity and composition in the free
666 troposphere and the boundary layer during INTEX-B, *Atmos. Chem. Phys.*, 10, 6627-6644, 2010.

667 Robinson, N. H., Hamilton, J. F., Allan, J. D., Langford, B., Oram, D. E., Chen, Q., Docherty, K., Farmer, D. K.,
668 Jimenez, J. L., Ward, M. W., Hewitt, C. N., Barley, M. H., Jenkin, M. E., Rickard, A. R., Martin, S. T., McFiggans,
669 G., and Coe, H.: Evidence for a significant proportion of Secondary Organic Aerosol from isoprene above a
670 maritime tropical forest, *Atmos. Chem. Phys.*, 11, 1039-1050, 2011.

671 Rose, C., Sellegri, K., Asmi, E., Hervo, M., Freney, E., Colomb, A., Junninen, H., Duplissy, J., Sipilä, M.,
672 Kontkanen, J., Lehtipalo, K., and Kulmala, M.: Major contribution of neutral clusters to new particle formation at
673 the interface between the boundary layer and the free troposphere, *Atmos. Chem. Phys.*, 15, 3413-3428, 2015.

674 Schroder, F., Karcher, B., Fiebig, M., and Petzold, A.: Aerosol states in the free troposphere at northern
675 midlatitudes, *J. Geophys. Res. Atmos.*, 107, 8126-8133, 2002.

676 Schurman, M. I., Lee, T., Sun, Y., Schichtel, B. A., Kreidenweis, S. M., and Collett Jr, J. L.: Investigating types and
677 sources of organic aerosol in Rocky Mountain National Park using aerosol mass spectrometry, *Atmos. Chem. Phys.*,
678 15, 737-752, 2015.

679 Setyan, A., Zhang, Q., Merkel, M., Knighton, W. B., Sun, Y., Song, C., Shilling, J. E., Onasch, T. B., Herndon, S.
680 C., Worsnop, D. R., Fast, J. D., Zaveri, R. A., Berg, L. K., Wiedensohler, A., Flowers, B. A., Dubey, M. K., and
681 Subramanian, R.: Characterization of submicron particles influenced by mixed biogenic and anthropogenic
682 emissions using high-resolution aerosol mass spectrometry: results from CARES, *Atmos. Chem. Phys.*, 12, 8131-
683 8156, 2012.

684 [Sorooshian, A., Crosbie, E., Maudlin, L. C., Youn, J.-S., Wang, Z., Shingler, T., Ortega, A. M., Hersey, S., and](#)
685 [Woods, R. K.: Surface and airborne measurements of organosulfur and methanesulfonate over the western United](#)
686 [States and coastal areas. *Journal of Geophysical Research: Atmospheres*, 120, 8535-8548, 2015.](#)

687 Stohl, A., Trainer, M., Ryerson, T. B., Holloway, J. S., and Parrish, D. D.: Export of NO_y from the North American
688 boundary layer during 1996 and 1997 North Atlantic Regional Experiments, *J. Geophys. Res. Atmos.*, 107, 4131-
689 4139, 2002.

- 690 Sun, Y., Zhang, Q., Macdonald, A. M., Hayden, K., Li, S. M., Liggio, J., Liu, P. S. K., Anlauf, K. G., Leitch, W.
691 R., Steffen, A., Cubison, M., Worsnop, D. R., van Donkelaar, A., and Martin, R. V.: Size-resolved aerosol chemistry
692 on Whistler Mountain, Canada with a high-resolution aerosol mass spectrometer during INTEX-B, *Atmos. Chem.*
693 *Phys.*, 9, 3095-3111, 2009.
- 694 Sun, Y. L., Zhang, Q., Schwab, J. J., Yang, T., Ng, N. L., and Demerjian, K. L.: Factor analysis of combined organic
695 and inorganic aerosol mass spectra from high resolution aerosol mass spectrometer measurements, *Atmos. Chem.*
696 *Phys.*, 12, 8537-8551, 2012.
- 697 Takahama, S., Schwartz, R. E., Russell, L. M., Macdonald, A. M., Sharma, S., and Leitch, W. R.: Organic
698 functional groups in aerosol particles from burning and non-burning forest emissions at a high-elevation mountain
699 site, *Atmos. Chem. Phys.*, 11, 6367-6386, 2011.
- 700 [Taylor, N. F., Collins, D. R., Lowenthal, D. H., McCubbin, I. B., Hallar, A. G., Samburova, V., Zielinska, B.,](#)
701 [Kumar, N., and Mazzoleni, L. R.: Hygroscopic growth of water-soluble organic carbon isolated from atmospheric](#)
702 [aerosol collected at US national parks and Storm Peak Laboratory, *Atmos. Chem. Phys.*, 17, 2555-2571, 2017.](#)
- 703 Timonen, H., Jaffe, D. A., Wigder, N., Hee, J., Gao, H., Pitzman, L., and Cary, R. A.: Sources of carbonaceous
704 aerosol in the free troposphere, *Atmos. Environ.*, 92, 146-153, 2014.
- 705 Timonen, H., Wigder, N., and Jaffe, D.: Influence of background particulate matter (PM) on urban air quality in the
706 Pacific Northwest, *J. Environ. Manage.*, 129, 333-340, 2013.
- 707 Tröstl, J., Herrmann, E., Frege, C., Bianchi, F., Molteni, U., Bukowiecki, N., Hoyle, C. R., Steinbacher, M.,
708 Weingartner, E., Dommen, J., Gysel, M., and Baltensperger, U.: Contribution of new particle formation to the total
709 aerosol concentration at the high-altitude site Jungfrauoch (3580 m asl, Switzerland), *J. Geophys. Res. Atmos.*,
710 121, 11,692-611,711, 2016.
- 711 [Tunved, P., Ström, J., and Krejci, R.: Arctic aerosol life cycle: linking aerosol size distributions observed between](#)
712 [2000 and 2010 with air mass transport and precipitation at Zeppelin station, Ny-Ålesund, Svalbard, *Atmos. Chem.*](#)
713 [Phys., 13, 3643-3660, 2013.](#)
- 714 Ulbrich, I. M., Canagaratna, M. R., Zhang, Q., Worsnop, D. R., and Jimenez, J. L.: Interpretation of organic
715 components from Positive Matrix Factorization of aerosol mass spectrometric data, *Atmos. Chem. Phys.*, 9, 2891-
716 2918, 2009.
- 717 Van Dingenen, R., Putaud, J. P., Martins-Dos Santos, S., and Raes, F.: Physical aerosol properties and their relation
718 to air mass origin at Monte Cimone (Italy) during the first MINATROC campaign, *Atmos. Chem. Phys.*, 5, 2203-
719 2226, 2005.
- 720 [Wagner, N. L., Brock, C. A., Angevine, W. M., Beyersdorf, A., Campuzano-Jost, P., Day, D., de Gouw, J. A.,](#)
721 [Diskin, G. S., Gordon, T. D., Graus, M. G., Holloway, J. S., Huey, G., Jimenez, J. L., Lack, D. A., Liao, J., Liu, X.,](#)
722 [Markovic, M. Z., Middlebrook, A. M., Mikoviny, T., Peischl, J., Perring, A. E., Richardson, M. S., Ryerson, T. B.,](#)
723 [Schwarz, J. P., Warneke, C., Welti, A., Wisthaler, A., Ziemba, L. D., and Murphy, D. M.: In situ vertical profiles of](#)
724 [aerosol extinction, mass, and composition over the southeast United States during SENEX and](#)
725 [SEAC⁴RS: observations of a modest aerosol enhancement aloft, *Atmos. Chem. Phys.*, 15, 7085-7102,](#)
726 [2015.](#)
- 727 Wang, J., Krejci, R., Giangrande, S., Kuang, C., Barbosa, H. M., Brito, J., Carbone, S., Chi, X., Comstock, J., Ditas,
728 F., Lavric, J., Manninen, H. E., Mei, F., Moran-Zuloaga, D., Pohlker, C., Pohlker, M. L., Saturno, J., Schmid, B.,

729 Souza, R. A., Springston, S. R., Tomlinson, J. M., Toto, T., Walter, D., Wimmer, D., Smith, J. N., Kulmala, M.,
730 Machado, L. A., Artaxo, P., Andreae, M. O., Petaja, T., and Martin, S. T.: Amazon boundary layer aerosol
731 concentration sustained by vertical transport during rainfall, *Nature*, 539, 416-419, 2016.

732 Watts, S. F.: The mass budgets of carbonyl sulfide, dimethyl sulfide, carbon disulfide and hydrogen sulfide, *Atmos.*
733 *Environ.*, 34, 761-779, 2000.

734 Weiss-Penzias, P., Jaffe, D. A., Swartzendruber, P., Dennison, J. B., Chand, D., Hafner, W., and Prestbo, E.:
735 Observations of Asian air pollution in the free troposphere at Mount Bachelor Observatory during the spring of
736 2004, *J. Geophys. Res. Atmos.*, 111, D10304, 2006.

737 Worton, D. R., Goldstein, A. H., Farmer, D. K., Docherty, K. S., Jimenez, J. L., Gilman, J. B., Kuster, W. C., de
738 Gouw, J., Williams, B. J., Kreisberg, N. M., Hering, S. V., Bench, G., McKay, M., Kristensen, K., Glasius, M.,
739 Surratt, J. D., and Seinfeld, J. H.: Origins and composition of fine atmospheric carbonaceous aerosol in the Sierra
740 Nevada Mountains, California, *Atmos. Chem. Phys.*, 11, 10219-10241, 2011.

741 Xu, J., Zhang, Q., Shi, J., Ge, X., Xie, C., Wang, J., Kang, S., Zhang, R., and Wang, Y.: Chemical characteristics of
742 submicron particles at the central Tibetan Plateau: insights from aerosol mass spectrometry, *Atmos. Chem. Phys.*,
743 18, 427-443, 2018.

744 Young, D. E., Kim, H., Parworth, C., Zhou, S., Zhang, X., Cappa, C. D., Seco, R., Kim, S., and Zhang, Q.:
745 Influences of emission sources and meteorology on aerosol chemistry in a polluted urban environment: results from
746 DISCOVER-AQ California, *Atmos. Chem. Phys.*, 16, 5427-5451, 2016.

747 Zhang, L. and Jaffe, D. A.: Trends and sources of ozone and sub-micron aerosols at the Mt. Bachelor Observatory
748 (MBO) during 2004–2015, *Atmos. Environ.*, 165, 143-154, 2017.

749 Zhang, Q., Jimenez, J. L., Canagaratna, M. R., Allan, J. D., Coe, H., Ulbrich, I., Alfarra, M. R., Takami, A.,
750 Middlebrook, A. M., Sun, Y. L., Dzepina, K., Dunlea, E., Docherty, K., DeCarlo, P. F., Salcedo, D., Onasch, T.,
751 Jayne, J. T., Miyoshi, T., Shimojo, A., Hatakeyama, S., Takegawa, N., Kondo, Y., Schneider, J., Drewnick, F.,
752 Borrmann, S., Weimer, S., Demerjian, K., Williams, P., Bower, K., Bahreini, R., Cottrell, L., Griffin, R. J.,
753 Rautiainen, J., Sun, J. Y., Zhang, Y. M., and Worsnop, D. R.: Ubiquity and dominance of oxygenated species in
754 organic aerosols in anthropogenically-influenced Northern Hemisphere midlatitudes, *Geophys Res Lett*, 34, 6, 2007.

755 Zhang, Q., Jimenez, J. L., Canagaratna, M. R., Ulbrich, I. M., Ng, N. L., Worsnop, D. R., and Sun, Y. L.:
756 Understanding atmospheric organic aerosols via factor analysis of aerosol mass spectrometry: a review, *Anal*
757 *Bioanal Chem*, 401, 3045-3067, 2011.

758 Zhang, Q., Zhou, S., Collier, S., Jaffe, D., Onasch, T., Shilling, J., Kleinman, L., and Sedlacek, A.:
759 Understanding Composition, Formation, and Aging of Organic Aerosols in Wildfire Emissions via Combined
760 Mountain Top and Airborne Measurements. In: *Multiphase Environmental Chemistry in the Atmosphere*,
761 American Chemical Society (ACS) Books: Vol. 1299, 363-385, 2018.

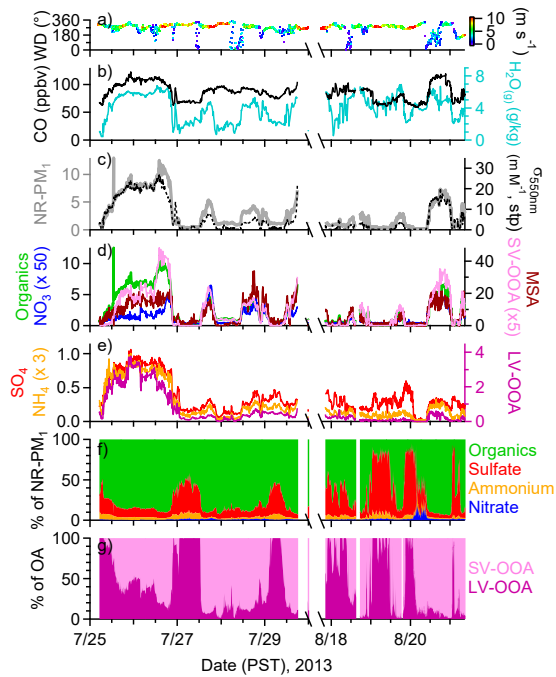
762 Zhou, S., Collier, S., Jaffe, D. A., Briggs, N. L., Hee, J., Sedlacek Iii, A. J., Kleinman, L., Onasch, T. B., and Zhang,
763 Q.: Regional influence of wildfires on aerosol chemistry in the western US and insights into atmospheric aging of
764 biomass burning organic aerosol, *Atmos. Chem. Phys.*, 17, 2477-2493, 2017.

765 Zhou, S., Collier, S., Xu, J., Mei, F., Wang, J., Lee, Y.-N., Sedlacek, A. J., Springston, S. R., Sun, Y., and Zhang,
766 Q.: Influences of upwind emission sources and atmospheric processing on aerosol chemistry and properties at a rural
767 location in the Northeastern U.S., *J. Geophys. Res. Atmos.*, 121, 6049-6065, 2016.

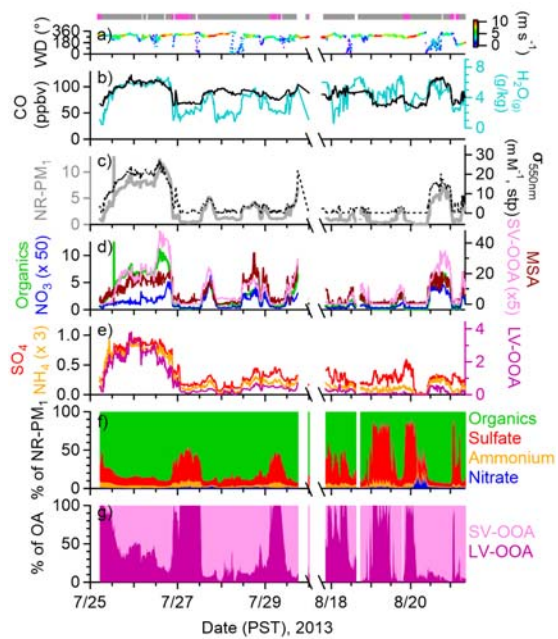
768 Zhu, Q., He, L. Y., Huang, X. F., Cao, L. M., Gong, Z. H., Wang, C., Zhuang, X., and Hu, M.: Atmospheric aerosol
769 compositions and sources at two national background sites in northern and southern China, *Atmos. Chem. Phys.*, 16,
770 10283-10297, 2016.

771 Zorn, S. R., Drewnick, F., Schott, M., Hoffmann, T., and Borrmann, S.: Characterization of the South Atlantic
772 marine boundary layer aerosol using an aerodyne aerosol mass spectrometer, *Atmos. Chem. Phys.*, 8, 4711-4728,
773 2008.

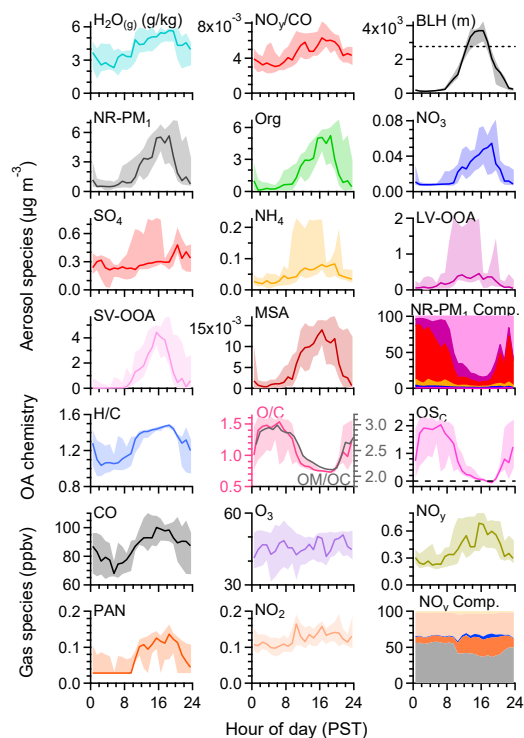
774



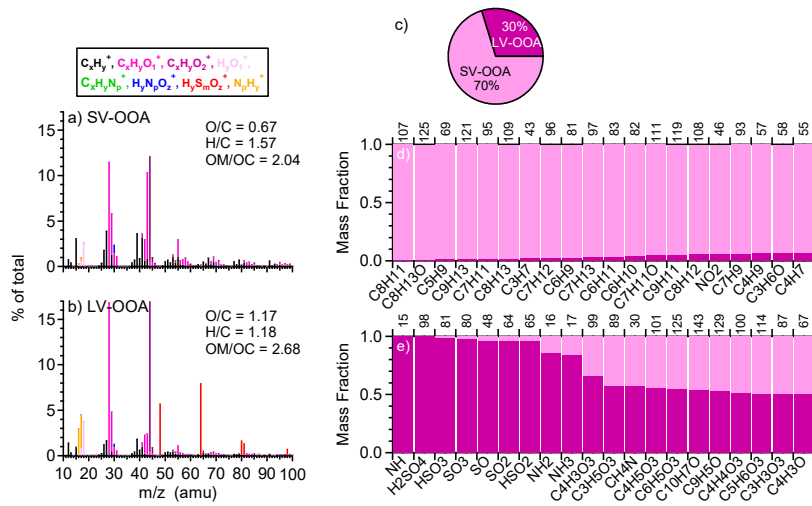
775



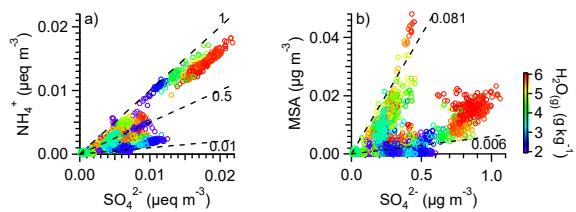
776
 777 **Fig. 1.** Observations during two clean periods in summer 2013. Time series of (a) wind direction (WD) colored
 778 by wind speed (WS in $m s^{-1}$), (b) mixing ratios of CO and water vapor (H_2O ($g kg^{-1}$)), (c - e) mass concentrations of NR-PM₁
 779 species and OA factors ($\mu g m^{-3}$), and organic equivalent mass concentration of SV-OOA and MSA ($ng m^{-3}$) at ambient
 780 conditions, and submicron aerosol light scattering at 550 nm (σ_{550nm}), (f) NR-PM₁ composition, and (g) OA
 781 composition. The indicator bars at the top of the graph are colored by air mass types: free troposphere (pink) and
 782 boundary layer influenced (gray).



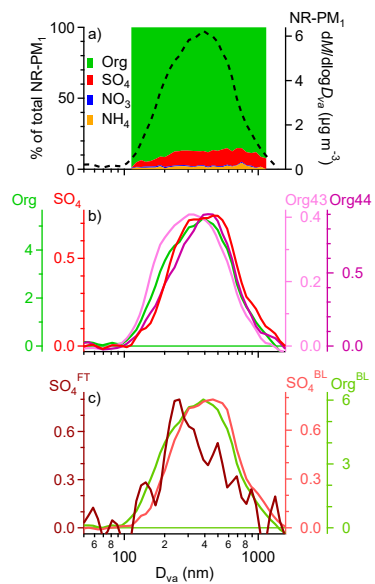
783
 784 **Fig. 2. Median diurnal** Diurnal cycles of the median values of water vapor ($H_2O_{(g)}$), NO_y/CO ratio (ppb/ppb),
 785 estimated boundary layer height (BLH), mass concentrations of NR-PM₁ species, elemental ratios of OA chemistry,
 786 and mixing ratios of gas species at MBO during the two clean periods shown in Fig. 1 at MBO. MSA is in organic
 787 equivalent mass concentrations summer 2013. Oxidation state of carbon (OS_C) = $2 O/C - H/C$. The shaded areas indicate
 788 the 75th and 25th percentiles. The diurnal cycle of NR-PM₁ composition displays the percent mass contributions, from
 789 top to bottom, of SV-OOA in light pink, LV-OOA in dark purple, sulfate in red, ammonium in orange, nitrate in blue,
 790 and chloride in purple. The diurnal cycle of NO_y composition displays the percent mixing ratio contributions, from
 791 top to bottom, of NO in yellow, NO₂ in light orange, nitrate in blue, PAN in dark orange, and NO_x (= $NO_y - NO -$
 792 $NO_2 - nitrate - PAN$) in grey. Dashed line in the BLH plot indicates the altitude of MBO (2763 m).



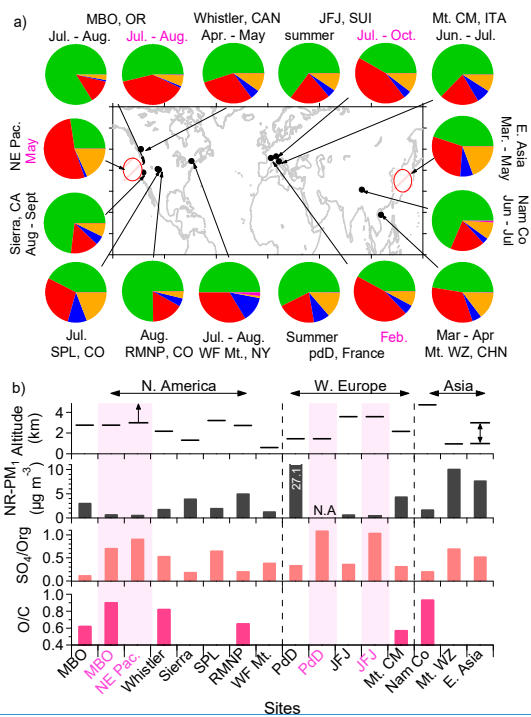
793
 794 **Fig. 3.** High resolution mass [spectrumspectra](#) of (a) SV-OOA and (b) LV-OOA colored by eight ion families.
 795 The elemental ratios of OA determined using the IA method are shown in the legends. (c) Average OA composition.
 796 (d-e) [Ion-signal](#)The distribution of signals between SV-OOA and LV-OOA. [Top for 20 most abundant ions with](#)
 797 [greater fraction in SV-OOA in \(d\) and those with greater fraction in LV-OOA in \(e\).](#) The nominal masses of the ions
 798 are shown on the top axes of (d) and (e).



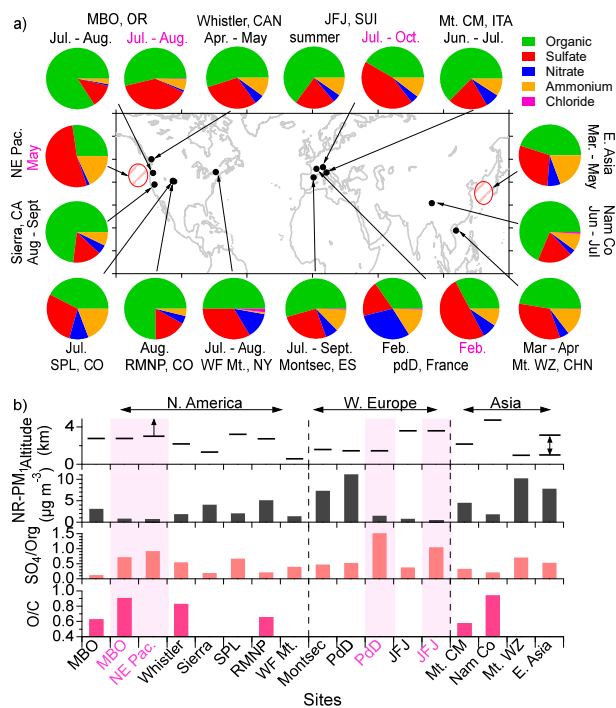
799
 800 **Fig. 4.** Scatter plots that compare (a) Ammonium ammonium molar equivalent concentration ($[\text{NH}_4^+]/18$) vs.
 801 sulfate molar equivalent concentration ($[\text{SO}_4^{2-}]/48$) and (b) MSA mass concentration vs. sulfate mass concentration.
 802 Data points are colored by water vapor mixing ratio. Dashed lines with different slopes are added for reference.



803
 804 **Fig. 5.** (a) Size-resolved aerosol composition on the left axis, average size distributions of total NR-PM₁ mass
 805 on the right. (b) Average mass-based size distributions of organics, sulfate, Org43, and Org44 during the clean periods.
 806 (c) Average mass-based size distributions of FT sulfate and BL influenced sulfate and organics. [The units for the y](#)
 807 [axes in \(b\) and \(c\) are \$\mu\text{g m}^{-3}\$.](#)



Formatted: Indent: First line: 0"



809
 810 **Fig. 6.** (a) Location of selected high-altitude mountain sites and aircraft measurements of regional background
 811 aerosols in the world and the chemical composition of NR-PM₁ (details are listed in Table S1 in the Supplement). Pie
 812 charts show the average chemical composition: organics (green), sulfate (red), nitrate (blue), ammonium (orange), and
 813 chloride (purple) of NR-PM₁. (b) Sampling altitude, average NR-PM₁ mass concentration, sulfate-to-organic mass
 814 ratio (SO₄/Org), and average O/C ratio of OA determined from using the Ambient-Aiken method for each site. Colors
 815 of the sampling period labels for pie charts in (a) and the bottom axis labels for sites in (b) indicate air
 816 according to air mass types: mixed BL/FT air (black) and FT air only (pink). Shaded pink bars in (b)
 817 indicate the FT air data.